

In-Situ Captures of AWS-1 LTE for Aeronautical Mobile Telemetry System Evaluation

**Eric D. Nelson
Duncan A. McGillivray**



Technical Report

In-Situ Captures of AWS-1 LTE for Aeronautical Mobile Telemetry System Evaluation

**Eric D. Nelson
Duncan A. McGillivray**



U.S. DEPARTMENT OF COMMERCE

Evelyn Remaley
Acting Assistant Secretary of Commerce for Communications and Information
National Telecommunications and Information Administration

March 2021

DISCLAIMER

Certain commercial equipment and materials are identified in this report to specify adequately the technical aspects of the reported results. In no case does such identification imply recommendation or endorsement by the National Telecommunications and Information Administration, nor does it imply that the material or equipment identified is the best available for this purpose.

PREFACE

The work described herein was performed as a result of a spectrum sharing project request submitted to the National Advanced Spectrum and Communications Test Network (NASCTN). The National Telecommunications and Information Administration (NTIA) is a founding charter member of NASCTN. This work was sponsored by Edwards Airforce Base, and conducted by NTIA's Institute for Telecommunication Sciences with participation by NIST, NASA, and MITRE. A summary of each organization's technical contributions follows the description of NASCTN.

The project underwent formal screening and approval by the NASCTN Steering Committee. A description of NASCTN and listing of Charter Members at the time of publication of this report follows.

NATIONAL ADVANCED SPECTRUM AND COMMUNICATIONS TEST NETWORK (NASCTN)

The mission of the National Advanced Spectrum and Communications Test Network (NASCTN) is to provide, through its members, a network for robust test processes and validated measurement data necessary to develop, evaluate and deploy spectrum sharing technologies that can improve access to the spectrum by both federal agencies and non-federal spectrum users.

NASCTN is a membership organization under a charter agreement. Members

- Facilitate and coordinate work with federal, academic, and industry spectrum users to rapidly and cooperatively facilitate spectrum sharing and co-existence studies;
- Work as a partnership to address the interests and equities of all spectrum stakeholders in a fair, equitable, and non-preferential manner; and
- Through sharing of technical resources, with consideration for cost, provide liaison and support to coordinate and leverage existing national capabilities supporting government, academic, and industry testing and evaluation known to improve and expedite spectrum sharing and co-existence.

Charter members at the time of publication of this report are (in alphabetical order):

- Department of Defense Chief Information Officer (DoD CIO)
- National Aeronautics and Space Administration (NASA)
- National Institute of Standards and Technology (NIST)
- National Oceanic and Atmospheric Administration (NOAA)
- National Science Foundation (NSF)
- National Telecommunications and Information Administration (NTIA)

The National Institute of Standards and Technology (NIST) hosts the NASCTN capability at the Department of Commerce Boulder Laboratories in Boulder, Colorado.

TECHNICAL CONTRIBUTORS

| Name | Organization | Primary Contribution Area |
|--------------------|---------------------|---|
| Eric Nelson | NTIA/ITS | Technical effort lead, test design, implementation, and execution; site survey, data analysis and review. |
| Kenneth Brewster | NTIA/ITS | Test implementation and execution |
| Frank Sanders | NTIA/ITS | Site survey and initial technical feasibility evaluation |
| Duncan McGillivray | NIST/CTL | Test design, implementation, and execution, data review, site survey and site prep |
| Melissa Midzor | NIST/CTL | Test coordination, test implementation, site survey |
| Adam Wunderlich | NIST/CTL | Guidance in data processing |
| William Young | MITRE | Project Technical Lead, test design |
| Kenneth Dudley | NASA | Telemetry systems configuration and applications |
| Claude (Lee) Joyce | NASA | Telemetry systems configuration and applications |

ACKNOWLEDGEMENTS

The authors would like to thank the many individuals and organization representatives that made valuable contributions towards the test effort.

First and foremost, we would like to thank Kip Temple of the US Air Force (USAF) for his guidance, feedback, and gracious hosting of the test team. His insights and accommodations allowed for a positive, efficient, and successful measurement campaign.

Second, we would like to thank NASA Langley Research Center's Claude (Lee) Joyce and Kenneth Dudley for their valuable contributions in configuring and controlling the Langley Research Antenna System, and providing detailed insights and context into telemetry operations in civil and Federal aviation fora.

Third, we thank Mark Lofquist (MITRE), Azizollah Kord (CTL,NIST), and Jason Coder (CTL, NIST) for in depth technical conversations and guidance towards test implementation.

Additionally, the authors recognize the programmatic representatives: Barbara Wheaton (Edwards Air Force Base), Keith Gremban (former NTIA/ITS Director), Charmaine Franck and Steven Harrah (NASA Langley Research Center), Mark Lofquist (DoD CIO liaison), and Melissa Midzor (NASCTN Program Manager).

Finally the effort wouldn't have been possible without the resources of Thomas O'Brien of the Test Resource Management Center and Thomas Taylor of the Department of Defense Chief Information Office.

CONTENTS

| | |
|--|-----|
| Disclaimer | i |
| Preface..... | ii |
| National Advanced Spectrum and Communications Test Network (NASCTN)..... | iii |
| Technical Contributors..... | iv |
| Acknowledgements..... | v |
| List of Figures | vii |
| List of Tables | x |
| Acronymns | xi |
| Executive Summary | xii |
| 1. Field Measurements | 1 |
| 1.1 Test Sites..... | 2 |
| 1.1.1 Edwards Air Force Base | 2 |
| 1.1.2 NASA Langley Research Center | 4 |
| 1.2 System G/T Determination | 4 |
| 1.3 RF Environment Survey | 7 |
| 1.4 Live Capture Procedure | 10 |
| 1.4.1 Phase 1: Single UE Emissions Capture Procedure | 10 |
| 1.4.2 Phase 2 Capture of Multiple UEs Through the Antenna Asset..... | 12 |
| 1.4.3 I/Q Recording Parameters..... | 13 |
| 1.5 Post-processing of Live Captures | 14 |
| 1.6 Selection of Waveforms for Bench Testing..... | 17 |
| 1.6.1 Multi-UE Waveforms | 17 |
| 1.6.2 Single UE Waveforms | 27 |
| 1.7 Further Signal Analysis Considerations | 29 |
| 2. Conclusions..... | 31 |
| 3. References..... | 32 |
| Appendix A : Waveform Examples..... | 33 |
| A.1 Selected Waveforms from the Edwards AFB (EAFB) Site..... | 33 |
| A.2 Single UE Waveforms | 40 |

LIST OF FIGURES

| | |
|--|----|
| Figure 1. Google Maps™ view of the EAFB, CA, collection site in context to the Air Force base. | 2 |
| Figure 2. Antenna 5 at the EAFB collection site. The sealed feed sections were inaccessible for noise diode based calibration procedures, thus a gain over thermal noise (G/T) measurement was performed. | 3 |
| Figure 3. System level diagram of the measurement campaign at EAFB. The antenna front end did not allow for examination, the conditioning of the RF signal was derived empirically through inspection with the PXA. | 3 |
| Figure 4. Google Maps™ view of the LRAS collection site in context to Hampton Roads area of Virginia. | 4 |
| Figure 5. Simplified block diagram of NASA/LaRC receive system. | 6 |
| Figure 6. Calibrated S-parameter measurements of the NTIA preselector as conducted in the field prior to deployment in the LRAS measurement setup. | 6 |
| Figure 7. Keysight N9030B Real-Time SA mode display. | 7 |
| Figure 8. Dish-mounted antenna camera display showing an LTE source, i.e. a vehicle on the Barstow-Bakersfield Highway. | 8 |
| Figure 9. Key azimuths traced to potential sources from which strong emissions were observed at EAFB. | 9 |
| Figure 10. Key azimuths traced to potential sources from which strong emissions were observed at NASA/LaRC. | 10 |
| Figure 11. Single UE in close proximity to the AMT antenna asset at EAFB (left) and NASA/LaRC (right). | 11 |
| Figure 12. Typical full bandwidth spectrogram over a 100 ms timeframe. | 15 |
| Figure 13. Channel power vs. time plot for a typical capture. | 16 |
| Figure 14. Typical spectrum contours plot for a 5 s timeframe. | 17 |
| Figure 15. Channel power per FFT for a 100 ms sliding window using 50 ms steps. | 18 |
| Figure 16. Channel power per FFT for a 500 ms sliding window using 50 ms steps. | 19 |
| Figure 17. Spectrogram of the first 100 ms in the waveform captured at EAFB along azimuth of 76°. | 20 |
| Figure 18. Spectrum contours of the first 1 s in the waveform captured at EAFB along azimuth of 76°. | 21 |
| Figure 19. Stationarity analysis, using a 500 ms window size, of the selected waveform captured at EAFB along azimuth of 76°. | 21 |
| Figure 20. Spectrogram of the first 100 ms in the waveform captured at EAFB along azimuth of 198°. | 22 |
| Figure 21. Spectrum contours of the first 1 s in the waveform captured at EAFB along azimuth of 198°. | 22 |
| Figure 22. Stationarity analysis, using a 500 ms window size, of the selected waveform captured at EAFB along azimuth of 198°. | 23 |
| Figure 23. Spectrogram of the first 100 ms in the waveform captured at NASA/LaRC along azimuth of 140°. | 24 |

| | |
|--|----|
| Figure 24. Spectrum contours of the full waveform 5 s captured at NASA/LaRC along azimuth of 140°..... | 25 |
| Figure 25. Stationarity analysis, using a 500 ms window size, of the selected waveform captured at NASA/LaRC along azimuth of 140°..... | 25 |
| Figure 26. Spectrogram of the first 100 ms in the waveform captured at NASA/LaRC along azimuth of 165°..... | 26 |
| Figure 27. Spectrum contours of the full waveform 5 s captured at NASA/LaRC along azimuth of 165°..... | 26 |
| Figure 28. Stationarity analysis, using a 500 ms window size, of the selected waveform captured at NASA/LaRC along azimuth of 165°..... | 27 |
| Figure 29. Spectrogram slice of time 0.7s to 0.8 s within the overall 5 s capture of a single UE waveform captured at EAFB. The UE was set to a targeted upload rate of 10 Mbps..... | 28 |
| Figure 30. Spectrum contours for the first second of the overall capture..... | 29 |
| Figure 31. Characteristics of lowpass filter..... | 30 |
| Figure 32. Full bandwidth spectrogram after bandpass filtering..... | 30 |
| | |
| Figure A-1. Spectrogram of the first 100 ms in the waveform captured at EAFB along azimuth of 76°..... | 33 |
| Figure A-2. Spectrum contours of the first 1 s in the waveform captured at EAFB along azimuth of 76°..... | 34 |
| Figure A-3. Stationarity analysis, using a 500 ms window size, of the selected waveform captured at EAFB along azimuth of 76°..... | 34 |
| Figure A-4. Spectrogram of the first 100 ms in the waveform captured at EAFB along azimuth of 198°..... | 35 |
| Figure A-5. Spectrum contours of the first 1 s in the waveform captured at EAFB along azimuth of 198°..... | 35 |
| Figure A-6. Stationarity analysis, using a 500 ms window size, of the selected waveform captured at EAFB along azimuth of 198°..... | 36 |
| Figure A-7. Spectrogram of the first 100 ms in the waveform captured at NASA/LaRC along azimuth of 140°..... | 37 |
| Figure A-8. Spectrum contours of the full waveform 5 s captured at NASA/LaRC along azimuth of 140°..... | 37 |
| Figure A-9. Stationarity analysis, using a 500 ms window size, of the selected waveform captured at NASA/LaRC along azimuth of 140°..... | 38 |
| Figure A-10. Spectrogram of the first 100 ms in the waveform captured at NASA/LaRC along azimuth of 165°..... | 38 |
| Figure A-11. Spectrum contours of the full waveform 5 s captured at NASA/LaRC along azimuth of 165°..... | 39 |
| Figure A-12. Stationarity analysis, using a 500 ms window size, of the selected waveform captured at NASA/LaRC along azimuth of 165°..... | 39 |

Figure A-13. Spectrogram slice of time 0.7s to 0.8 s within the overall 5 s capture of a single UE waveform captured at EAFB. The UE was set to a targeted upload rate of 10 Mbps. 40

Figure A-14. Spectrum contours for the first second of the overall capture..... 41

LIST OF TABLES

| | |
|---|----|
| Table 1. Total effective noise temperature computation. | 6 |
| Table 2. Requested and reported data rates from infield measurements. | 11 |
| Table 3. Vectors and number of captures performed at EAFB. Note the azimuth of 0 degree indicates due North..... | 12 |
| Table 4. Vectors and number of captures performed at LaRC. Note due North is indicated by an azimuth of 0 degree. | 13 |
| Table 5. LTE uplink band parameters and associated VSA capture settings. | 13 |

ACRONYMNS

| | |
|--------|--|
| 3GPP | 3 rd Generation Partnership Project |
| AFB | Air Force Base |
| AMT | Aeronautical Mobile Telemetry |
| AWGN | additive white Gaussian noise |
| AWS-1 | Advanced Wireless Services - 1 |
| AWS-3 | Advanced Wireless Services - 3 |
| CDF | cumulative density functions |
| EAFB | Edwards Air Force Base |
| EIRP | equivalent isotropic radiated power |
| FFT | fast Fourier transform |
| FIR | finite impulse response |
| G/T | gain over temperature |
| I/Q | in-phase/quadrature |
| IP | internet protocol |
| ITS | Institute for Telecommunication Sciences |
| LNA | low noise amplifier |
| LRAS | Langley Research Antenna System |
| LTE | long term evolution |
| NASA | National Aeronautics and Space Administration |
| NASCTN | National Advanced Spectrum and Communications Test Network |
| NIST | National Institute of Standards and Technology |
| NOAA | National Oceanic and Atmospheric Administration |
| NTIA | National Telecommunications and Information Administration |
| PXA | high performance signal analyzer |
| RB | resource block |
| RF | radio frequency |
| RTSA | real time spectrum analyzer |
| SNR | signal to noise ratio |
| UE | user equipment |
| VSA | vector signal analyzer |
| VSG | vector signal generator |
| WGS-84 | World Geodetic System 1984 |

EXECUTIVE SUMMARY

The Advanced Wireless Services - 3 (AWS-3) auction of 1755–1780 MHz for commercial mobile uplink use resulted in the loss of the lower band of aeronautical mobile telemetry (AMT) L-Band operations. Compression of operations into 1780–1850 MHz will cause more frequent adjacent channel operations at AMT facilities. To gauge the impact to AMT operations from mobile transmissions in the lower adjacent band, the program’s sponsor, Edwards AFB (EAFB), commissioned National Advanced Spectrum and Communications Test Network member organizations to perform an AMT receiver susceptibility study. The crux of the study is a comprehensive battery of laboratory tests in which representative AMT receivers are operated over their range of modes while subjected to a complement of synthesized, laboratory captured, and in situ captured Long Term Evolution (LTE) waveforms that exhibit adjacent band transmissions.

In-situ captures were obtained at both EAFB and NASA Langley Research Center (NASA/LaRC), yielding data from environmentally disparate locations. Since AWS-3 deployments at both locations had not occurred yet, transmissions at the upper end of the AWS-1 band (1710-1755 MHz) were used as a proxy. At both facilities, a site survey was first conducted to inform the collection approach of the in-situ captures. Primarily, the surveys yielded insights into AMT system characteristics and, as was necessary at NASA/LaRC, plans for implementing system modifications to permit follow-on measurements. In addition, measurement system parameters were determined and spectrum scans over the full range of antenna azimuths were performed to catalog locations with significant LTE user equipment (UE) uplink activity and received power.

During the second visit to each location, multiple captures of live uplink traffic at the aforementioned azimuths were completed. A direct measurement of system gain over thermal noise (G/T), which provides a benchmark for interpreting captured signals, was completed at EAFB. At NASA/LaRC measurements were performed so that G/T could be computed. Finally, as a measure of worst case channel loading conditions, a test UE (mobile phone) was configured to transmit at higher data transfer rates from which several captures into sidelobes of the antennas were completed.

The data were post-processed into spectrograms and instantaneous power versus time, spectrum power contour, and sliding window channel power plots to permit examination of their characteristics and suitability for subsequent bench testing. Several waveforms were selected for use in connectorized AMT receiver susceptibility studies. The waveforms selected for further testing exhibited:

- 1) Good stationarity of the 90th centile of power at the PXA input with a 500 ms window size
- 2) Dynamic range of the recorded UL signal at least 20 dB above the PXA noise floor
- 3) Subjective selection on diversity of LTE in-band activity and recording azimuth.

In-Situ Captures of AWS-1 LTE for Aeronautical Mobile Telemetry System Evaluation

Eric D. Nelson¹ and Duncan A. McGillivray²

This report describes the rationale, measurement methods, and analysis techniques for assessing Long Term Evolution (LTE) user equipment (UE) emissions in the Advanced Wireless Services - 1 (AWS-1) uplink band within the observable range of aeronautical mobile telemetry (AMT) installations at Edwards AFB (EAFB) and NASA Langley Research Center (NASA/LaRC). Site surveys and measurements were conducted to understand the AMT receiver systems' radio frequency (RF) characteristics and survey the local spectrum environment's UE activity through antenna azimuthal scans and test instrument bandwidths encompassing in-band and out-of-band emissions. Based on survey findings, select azimuths were revisited and numerous vector signal analyzer in-phase/quadrature (I/Q) captures of uncontrolled multiple UE over-the-air emissions were performed. A single controlled UE operating in a test mode facilitated captures for several data throughput rates of interest. Data post-processing techniques, analysis methods, and qualifying factors used to identify captures for inclusion in subsequent AMT receiver susceptibility bench top studies are detailed.

Keywords: azimuthal scans, AWS-1, vector signal analyzer, I/Q capture, spectrogram, uplink emissions, G/T, spectrum contours, stationarity analysis

1. FIELD MEASUREMENTS

Aeronautical mobile telemetry (AMT) bands have been compressed in their upper L-band operations from an allocation of 1755–1850 MHz to 1780–1850 MHz. In the near term, new entrants into the 1755–1780 MHz band are slated to be commercial AWS-3 3GPP LTE deployments. As a result, AMT stakeholders at Edwards AFB (EAFB) asked National Advanced Spectrum and Communications Test Network (NASCTN) members to investigate the adjacent band emissions impact of AWS-3 LTE on AMT receiver assets.

In order to investigate the behavior, engineers from NTIA, NIST, MITRE, and NASA conducted recordings of AWS-1 LTE activity to support a susceptibility study of AMT receivers. The activity of AWS-1 serves as a proxy for the eventual AWS-3 deployments.

The purpose of recording AWS-1 emissions through the AMT antenna asset (instead of a general-purpose antenna and receive system, for example) is to replicate AMT operational conditions and system configurations to gauge the expected effects of AWS-3 emissions when

¹ The author is with the Institute for Telecommunication Sciences, National Telecommunications and Information Administration, U.S. Department of Commerce, Boulder, CO 80305.

² The author is with the Communications Technology Laboratory, National Institute of Standards and Technology, Boulder, CO 80305.

deployed. Relevant conditions and configurations include parabolic dish antenna directivity, low antenna elevation angles, and the influence of the receive chain, i.e. front-end filter, low noise amplifier (LNA), and receive multi-couplers. The effects of adjacent band emissions from single UE emissions and from multiple UEs were observed.

Site surveys and RF environment recordings were conducted at both EAFB (see Figure 1) and the NASA Langley Research Center (NASA/LaRC) (see Figure 4). During both site surveys we found a carrier operating in the AWS-1 portion of the LTE Band 4, or in Band 66 with an allocation of 20 MHz at a center frequency of 1735 MHz. At the time of the signal recording measurement campaign, the base station was identified as a Band 66 as reported by the test UE.

For the data acquisition we used a Keysight PXA Model N9030B spectrum analyzer which supports traditional swept frequency, real time spectrum analyzer (RTSA), and vector signal analyzer (VSA) modes of operation.

1.1 Test Sites

1.1.1 Edwards Air Force Base

The EAFB collection site was at Building 4795, using Antenna 5 (34.970400 N, 117.932000 W, 831.19 m WGS-84).



Figure 1. Google Maps™ view of the EAFB, CA, collection site in context to the Air Force base.



Figure 2. Antenna 5 at the EAFB collection site. The sealed feed sections were inaccessible for noise diode based calibration procedures, thus a gain over thermal noise (G/T) measurement was performed.

The EAFB AMT system (see Figure 3) consists of the antenna and its feed structure, which incorporates an L-band bandpass filter, with a passband of approximately 1370–2560 MHz. The signal is then routed via RF coaxial cable into the telemetry site, where the signal is piped into a receive multi coupler for distribution to the AMT receivers and general purpose test equipment used for channel monitoring.

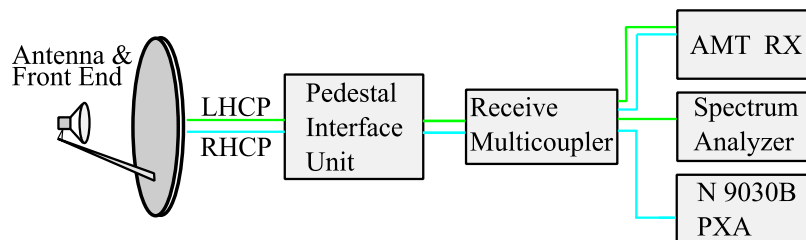


Figure 3. System level diagram of the measurement campaign at EAFB. The antenna front end did not allow for examination, the conditioning of the RF signal was derived empirically through inspection with the PXA.

The research team was furnished with a test port of the right hand circular polarization output of the receive multi coupler in the equipment rack adjacent to the associated AMT receiver and

monitoring test equipment. The test point was near the connection plane of the AMT receiver and expected to have near identical signal conditioning as would be experienced by the AMT receiver.

1.1.2 NASA Langley Research Center

The NASA/LaRC asset for the collection campaign was the Langley Research Antenna System (LRAS), located on top of the Hanger facility (at 37.085348 N, 76.376942 W), in Hampton VA.



Figure 4. Google Maps™ view of the LRAS collection site in context to Hampton Roads area of Virginia.

The LRAS system consists of a 3 m dish antenna with a front feed section in the S-band and C-band. For the purpose of this measurement campaign (see Figure 5 for the system diagram), the S-band feed was modified to pass right hand circularly polarized signal components into an external preselector (passband of 1700–1770 MHz, 37.2 dB gain); the C-band feed was bypassed. The signal out of the preselector was routed to the control room via coaxial RF cable and subsequently injected into the PXA for acquisition. The coaxial RF cable loss and length was characterized by terminating the control room side with a short. A reflection and distance to fault measurement was performed with a handheld network analyzer. The cable yielded a pathloss of 13 dB and a distance to fault measurement of 127 m (distance measurement is uncorrected for the dielectric constant for the cable).

The LRAS system diagram is outlined in Figure 5.

1.2 System G/T Determination

At EAFB access to the antenna feed was not available to facilitate a Y-factor calibration using a noise diode. Instead, the PXA was connected to the test port as described in Section 1.1.1. Noise

powers were measured using the sun and sky as sources. The system G/T (in dB/K) at 1755 MHz was calculated using the following equation [3].

$$G/T = 10 \log \left(\frac{8\pi k(Y - 1)}{\Phi \lambda^2} \right) \quad (1)$$

where k is Boltzmann's constant: $1.3806 \times 10^{-23} \frac{\text{m}^2 \text{kg}}{\text{s}^2 \text{K}}$, Φ is the solar power flux density $\left(\frac{\text{W}}{\text{m}^2}\right)$, λ is the wavelength, and Y is the (linear) Y-factor computed using the mean power (in mW) measured by orienting the antenna at the sun, P_{hot} , and at a cold section of sky, P_{cold} .

$$Y = \frac{P_{hot}}{P_{cold}} \quad (2)$$

The solar flux density of $5.77 \times 10^{-21} \frac{\text{W}}{\text{m}^2}$ was obtained by interpolating between measurements taken at the Sagamore Hill solar observatory in Massachusetts provided by the NOAA's Space Weather Prediction Center for 1415 and 2695 MHz. The hot and cold sky power measurements were -105 and -112.5 dBm, respectively. Converting those to mW and calculating yields a G/T of 9.8 dB/K.

At NASA/LARC the system configuration was modified to facilitate testing. See Figure 5 for a simplified block diagram of the configuration. A jumper cable was connected to one of the outputs of a 90° hybrid coupler on the antenna which fed directly to the dish's rotary joint. From there the signal passed down to the pedestal interface unit. The existing fiber optic module in the pedestal interface unit, which normally transfers the signal at optical frequencies to the control room, was bypassed with another coaxial jumper to the ITS custom preselector. The ITS preselector limits the signal energy to LTE bands of interest and applies gain to overcome loss in the acquisition system. The preselector consists of a manually tuneable bandpass filter and an LNA; the joint components were characterized (see Figure 6) prior to insertion into the test circuit. The preselector's manually tuneable bandpass filter has an insertion loss of approximately 0.4 dB. The measured net gain of the preselector, i.e. bandpass filter and LNA, was 37.2 dB at 1745 MHz, so the LNA gain is approximately 37.6 dB.

Net gain from the hybrid coupler output to the PXA (Cpl→Rx) and from the input of the preselector to the PXA (Pre→Rx) was measured using the Y-factor method and was 16.0 dB and 20.5 dB, respectively. Therefore, the loss from (Cpl→Pre) was 4.5 dB. The net feed loss (Ant→LNA) is required to calculate G/T. Taking into account the 90° hybrid coupler's specified 3.0 dB insertion loss and the bandpass filter's 0.4 dB of insertion loss yields: $3.0 + 4.5 + 0.4 = 7.9$ dB. We also require the cable loss from the output of the preselector to the PXA, which is $37.2 - 20.5 = 16.7$ dB.

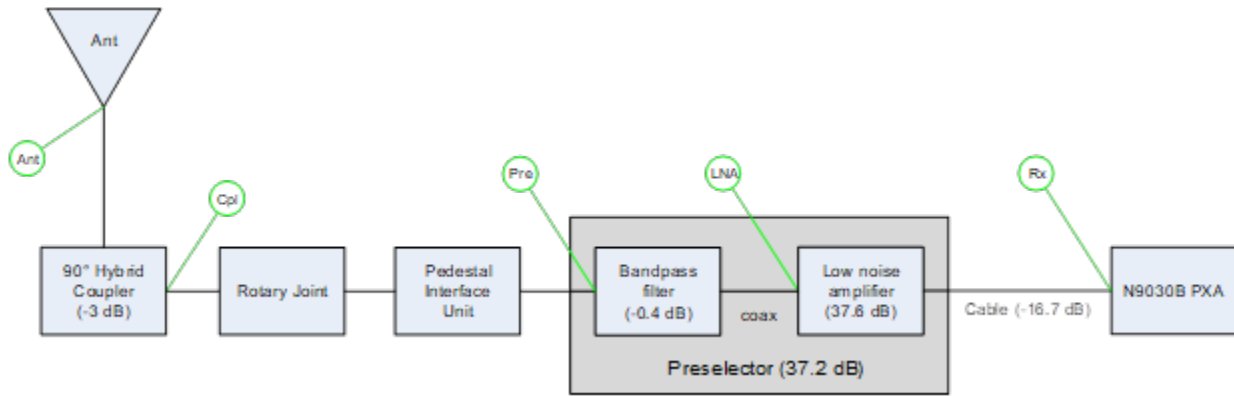


Figure 5. Simplified block diagram of NASA/LaRC receive system.

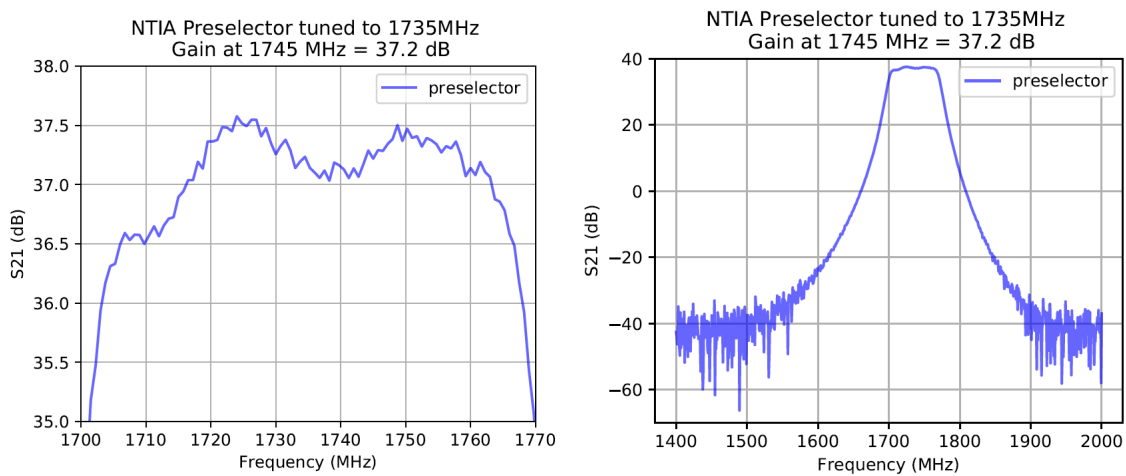


Figure 6. Calibrated S-parameter measurements of the NTIA preselector as conducted in the field prior to deployment in the LRAS measurement setup.

The calculated effective system noise temperature for the NASA/LaRC system is thus 345 K as detailed in Table 1.

Table 1. Total effective noise temperature computation.

| Component | Gain (dB) | g (linear) | f (linear) | F (dB) | T (K) | T _{LNA} (K) |
|-----------|-----------|------------|------------|--------|---------|----------------------|
| Antenna | 31.8 | | | | 150 | 24.33 |
| Feed | -7.9 | 0.16 | 6.17 | 7.90 | 1498.1 | 242.97 |
| LNA | 37.6 | 5754.40 | 1.19 | 0.75 | 54.7 | 54.67 |
| Cable | -16.7 | 0.02 | 46.77 | 16.70 | 13274.3 | 2.31 |
| Receiver | | | 10.00 | 10.00 | 2610.0 | 21.21 |
| Total | | | | | | 345.48 |

And the calculated G/T for this system is

$$\frac{G}{T} = (31.8 - 7.9) - 10 \log(345.48) = -1.5 \text{ dB/K}$$

The NASA/LaRC system G/T was substantially lower than that measured at EAFB because sub-optimal system configuration changes were required to facilitate testing. The primary driver was the 7.9 dB of loss introduced by the feed section between the antenna terminal and the LNA input.

1.3 RF Environment Survey

At both EAFB and NASA/LaRC multiple 0° to 360° azimuthal scans with the antenna at 0° elevation were conducted. The PXA was set to real time spectrum analysis mode, which displays full-bandwidth real-time fast Fourier transforms (FFTs), to facilitate observations of transmissions in time intervals as low as 1 ms. An example trace of the real-time observed spectrum is shown in Figure 7. Multiple full azimuthal scans were performed, and strong sources of AWS-1 LTE uplink emissions and their corresponding azimuths were logged. Recordkeeping was simplified by videotaping the PXA display as an operator read off the azimuth values in 5 degree increments.

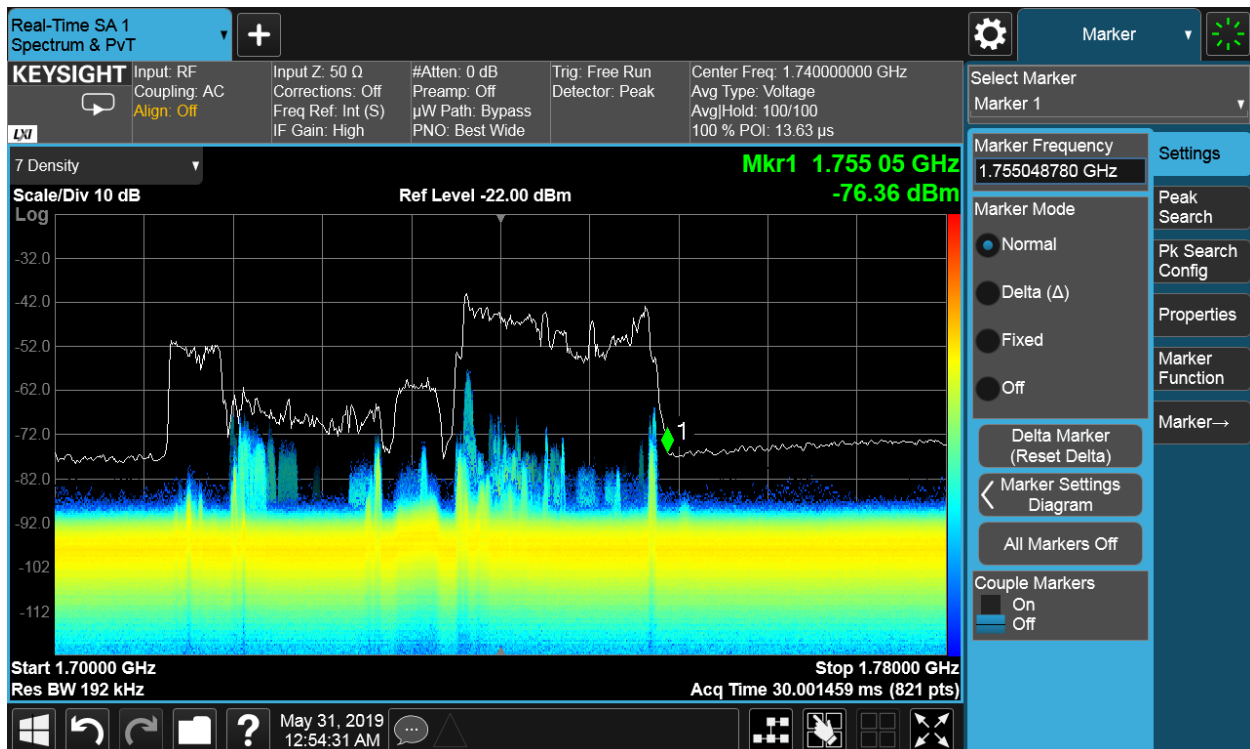


Figure 7. Keysight N9030B Real-Time SA mode display.

Identification of likely sources of emissions was attempted by tracing azimuths in Google Earth™ to nearby buildings, developed residential areas, or cities. At EAFB, a display in the

AMT control station from an on-axis dish mounted camera aided in source identification. A photograph of the control station display is shown in Figure 8. Sources of strong transmissions—more than 20 dB SNR—included an adjacent building, the flight line, buildings adjacent to the flight line, base housing, vehicles on the Barstow-Bakersfield Highway on the north border of the base, and all nearby cities.

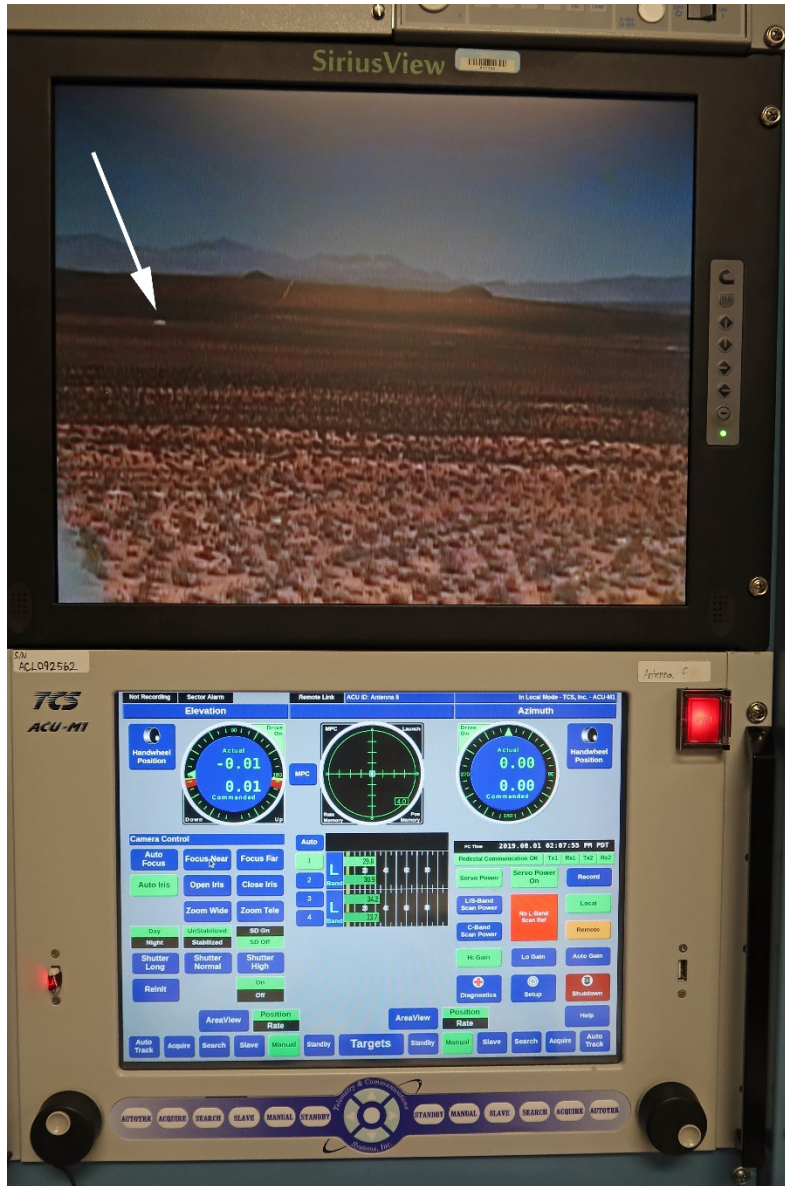


Figure 8. Dish-mounted antenna camera display showing an LTE source, i.e. a vehicle on the Barstow-Bakersfield Highway.



Figure 9. Key azimuths traced to potential sources from which strong emissions were observed at EAFB.

Likewise, an azimuth map prepared during the NASA/LaRC site survey showed several azimuths of interest. See Figure 10.



Figure 10. Key azimuths traced to potential sources from which strong emissions were observed at NASA/LaRC.

1.4 Live Capture Procedure

Live captures were conducted in two phases.

Phase 1: the acquisition of a single UE uplink signal broadcast under varying upload rates in near proximity to the AMT antenna asset, while in the back lobe or side lobe of the AMT antenna to prevent system overload.

Phase 2: the acquisition of uplink emissions of multiple UEs along the vectors of interest identified in the RF environment survey.

1.4.1 Phase 1: Single UE Emissions Capture Procedure

Researchers affixed a single phone in portrait orientation on a tripod and placed the tripod approximately 12 m from the antenna pedestal at EAFB, and approximately 50 m from the LRAS at NASA/LaRC. Both standoff distances are indicative of separation to the antenna asset by site personnel. Figure 11 shows photographs from the in-situ measurement of the single UE.



Figure 11. Single UE in close proximity to the AMT antenna asset at EAFB (left) and NASA/LaRC (right).

The UE was attached to a commercial cellular provider at a center frequency of 1745 MHz and 20 MHz allocation bandwidth, suggesting an AWS-1 deployment at Band 66, as identified by a third party open source cellular app, CellMapper, on the UE. In order to ensure continued attachment to the cellular providers in the frequency band of interest, we configured the non-volatile memory of the UE to only allow for attachments to Band 4 and Band 66 allocations.

The UE was configured to transmit UDP packets using Magic iPerf, an open source software implementation that allows for measuring achievable data rates on an IP network. The software was scripted to broadcast to an open server within the Continental US at target data rates using UDP traffic shown in Table 2.

Table 2. Requested and reported data rates from infield measurements.

* inconsistent condition, where only one of the tests was able to achieve the requested data rate.

| Requested data rate | Reported data rate | No of tests |
|---------------------|--------------------|-------------|
| 100 kbps | 100.5 kbps | 4 |
| 1 Mbps | 999.6 kbps | 3 |
| 5 Mbps | 4997.8 kbps | 2 |
| 10 Mbps | 9962.1 kbps | 2 |
| 20 Mbps | 19578.4 kbps | 2 |
| 50 Mbps | 49294.2 kbps* | 2 |

To limit the influence of emissions not from the test UE, at EAFB the AMT antenna was trained on an azimuth with limited UE activity in the band of interest, and the elevation optimized for dynamic range. The UE setup was in the back lobe of the antenna so as not to overload the antenna frontend LNA. Researchers set the UE into a broadcast mode while researchers inside the AMT facility verified observing the RF activity on the PXA which monitored RF spectrum at the plane of the receiver. Starting at an elevation of 0 degrees and raising the AMT antenna elevation angle allowed for optimizing the dynamic range of the acquisition. The AMT antenna position remained in the optimized position for the remainder of the single UE acquisitions.

At NASA/LaRC, the UE was set into broadcast mode and the AMT antenna azimuth was slewed until an optimized dynamic range was observed. The UE coupling mechanism was in a sidelobe of the antenna. The antenna’s position was then set for the remainder of the single UE acquisitions.

Single UE test acquisition sequence:

- 1) Place UE in “Airplane” mode to not allow for signal broadcasts.
- 2) Verify non-activity on the PXA.
- 3) Configure the Magic iPerf code to broadcast at a select upload rate.
- 4) Disable “Airplane” mode on the UE and start the Magic iPerf broadcast.
- 5) Verify RF activity on the real-time spectrum analyzer.
- 6) Record the RF activity in I/Q format on the PXA for 5 seconds
- 7) Place the UE in “Airplane” mode.
- 8) Save I/Q data to external hard drive.

1.4.2 Phase 2 Capture of Multiple UEs Through the Antenna Asset

I/Q recordings were performed by training the antenna asset to the vectors identified in the RF environment survey. The captures contain recordings of 5 seconds of RF activity. Some vectors with strong activity were recorded multiple times (see Tables 3 and 4).

Table 3. Vectors and number of captures performed at EAFB. Note the azimuth of 0 degree indicates due North.

| Azimuth | Elevation | # of Captures | |
|-----------------|-----------|---------------|-------|
| | | Day 1 | Day 2 |
| 0° | 0° | 4 | 2 |
| 76° | 0° | 2 | 3 |
| 153° | 0° | 4 | 8 |
| 176° | 0.7° | - | 5 |
| 198° | 0° | 5 | 3 |
| 292° | 0° | 3 | 3 |
| 305° | 1.4° | - | 2 |
| Subtotal | | 44 | |

Table 4. Vectors and number of captures performed at LaRC. Note due North is indicated by an azimuth of 0 degree.

| Azimuth | Elevation | # of Captures | |
|-----------------|-----------|---------------|-------|
| | | Day 1 | Day 2 |
| 5° | 0° | - | 2 |
| 15° | 0° | - | 2 |
| 87° | 0° | - | 2 |
| 92° | 0° | - | 2 |
| 135° | 0° | 9 | 2 |
| 140° | 0° | 4 | 2 |
| 145° | 0° | 7 | 2 |
| 150° | 0° | - | 2 |
| 155° | 0° | 5 | 2 |
| 165° | 0° | - | 2 |
| 223° | 0° | - | 2 |
| 257° | 0° | - | 2 |
| 292° | 0° | - | 2 |
| 337° | 0° | - | 2 |
| Subtotal | | 53 | |

1.4.3 I/Q Recording Parameters

PXA-based I/Q recordings were accomplished using a system developed to measure aggregate UE emissions in an LTE uplink band of interest. The system’s design and characteristics as well as a general description of standard data post-processing techniques are documented in a separate Technical Memorandum [1]. For the aggregate emissions application, PXA settings are tailored to the applicable bandwidth settings such that the sampling rate and FFT bin count consistently yield 15 kHz FFT bins, as is optimal for captures of LTE signals. Standard parameters for various LTE allocation sizes are shown in Table 5.

Table 5. LTE uplink band parameters and associated VSA capture settings.

| | | | | | |
|----------------------------------|------|-------|-------|-------|-------|
| Channel Bandwidth (MHz) | 5.0 | 10.0 | 15.0 | 20.0 | 30.0 |
| Occupied Bandwidth (MHz) | 4.5 | 9.0 | 12.0 | 18.0 | 24.0 |
| Number of PRBs | 25 | 50 | 75 | 100 | 150 |
| Sampling Frequency (MHz) | 7.68 | 15.36 | 23.04 | 30.72 | 46.08 |
| FFT size | 512 | 1024 | 1536 | 2048 | 3072 |
| Sub-carrier spacing (kHz) | 15 | | | | |
| VSA Span (MHz) | 6 | 12 | 18 | 24 | 36 |

At both EAFB and NASA/LaRC the AWS-1 D/E/F blocks which cover 1735-1755 MHz on the uplink were occupied by a 20 MHz LTE channel bandwidth. Rather than capturing in a 24 MHz span normally used for this bandwidth, a 36 MHz span was used, since wider capture bandwidths were desired to increase the observability of upper and lower adjacent out of band emissions. With the center frequency fixed at 1745 MHz, the RTSA span was increased to 36 MHz, and 3072 point FFTs were employed in post-processing. The center 1200 bins of each FFT then corresponded to the 100 PRBs in the occupied bandwidth of 18 MHz.

It should be noted that the PXA's RTSA mode restricts the displayed bandwidth to the indicated span, which is equal to the sampling rate divided by 1.28, since anti-aliasing filtering engages at the span edges and the instrument's absolute amplitude accuracy of ± 0.48 dB³ is not specified outside that range. This effect is noticeable as a roll off of noise floor on both sides of full bandwidth spectrograms. Figure 12 shows this effect as "dark blue" banding at the extreme frequency edges that is independent of filter roll off effects shown in Figure 6.

1.5 Post-processing of Live Captures

Spectrograms, channel power versus time, and spectrum contour plots were produced for each capture.

The spectrogram plots (see Figure 12) display the entire PXA capture bandwidth including frequencies outside the calibrated 36 MHz span which is essential for ascertaining the presence of strong out of band emissions which could cause system overload. The spectrogram is generated by reshaping the N sample long I/Q capture into a 3072 x (N/3072) array. Using Welch's method [2] with zero overlap we compute the FFT for each of the N/3072 rows of the array yielding power in mW/15 kHz. There are $46.08 \times 10^6 \frac{Sa}{s} \times \frac{1 FFT}{3072 Sa} = 15000 \frac{FFT}{s}$ or 15 FFT/ms. The result is saved in mW for later post-processing but converted to dBm for the spectrogram plot. To sufficiently resolve UE transmissions a 100 ms time span served as a practical limit, with 50 plots being necessary to view the full ensemble of spectrograms for a 5 second capture.

³ Keysight X-Series Signal Analyzers: PXA Specification Guide, available at: <http://literature.cdn.keysight.com/litweb/pdf/N9030-90017.pdf>

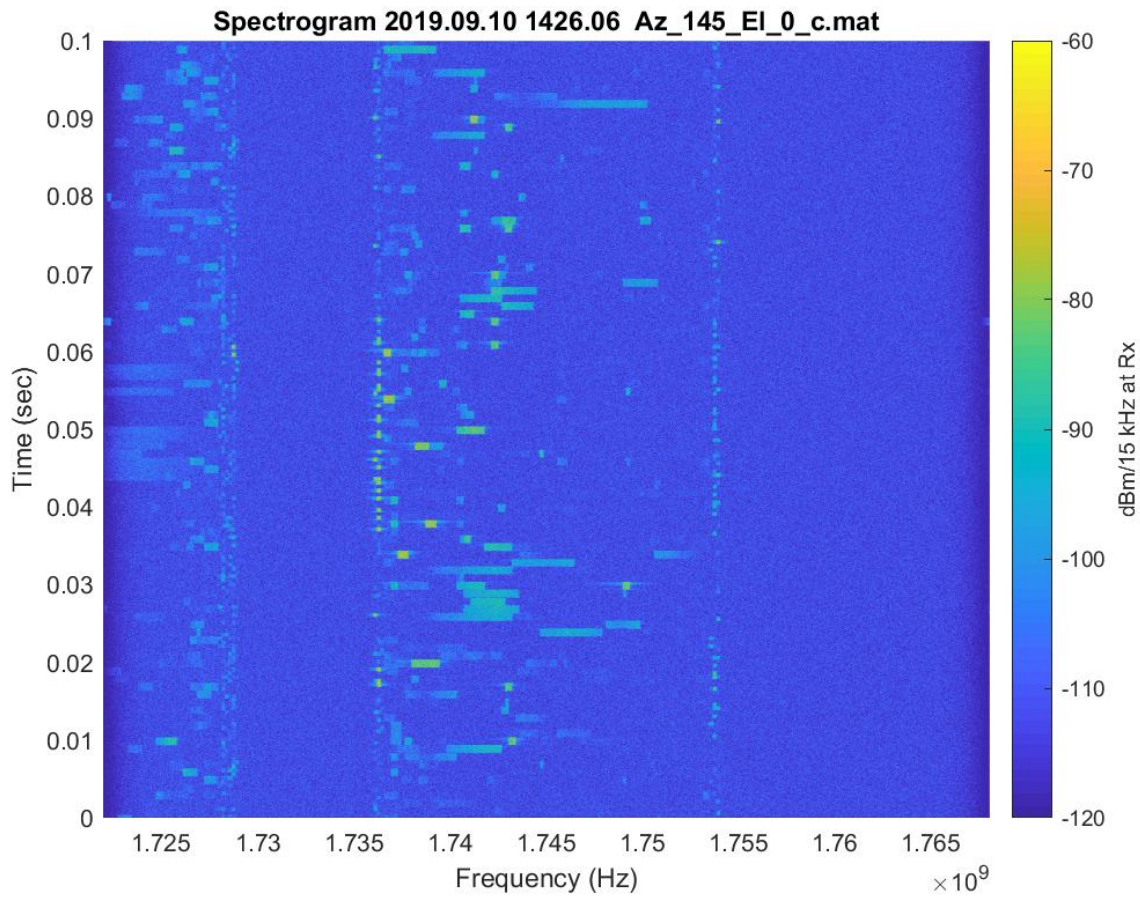


Figure 12. Typical full bandwidth spectrogram over a 100 ms timeframe.

To maximize dynamic range the PXA's input range power was adjusted, with only a few exceptions, to the instrument's most sensitive setting of -42 dBm. Following the first site survey at EAFB, after the data had been post-processed, we observed a number of short duration channel power excursions which caused overloads in a number of the captures. To ascertain whether captures were impacted by overload conditions and to permit the judicious use of segments of those captures which were not subject to overload, we also produced total channel power vs. time plots like that shown in Figure 13. These were generated by finding the peak power in 1 ms intervals within the full bandwidth time domain I/Q sequence and plotting the max power in each interval vs. time.

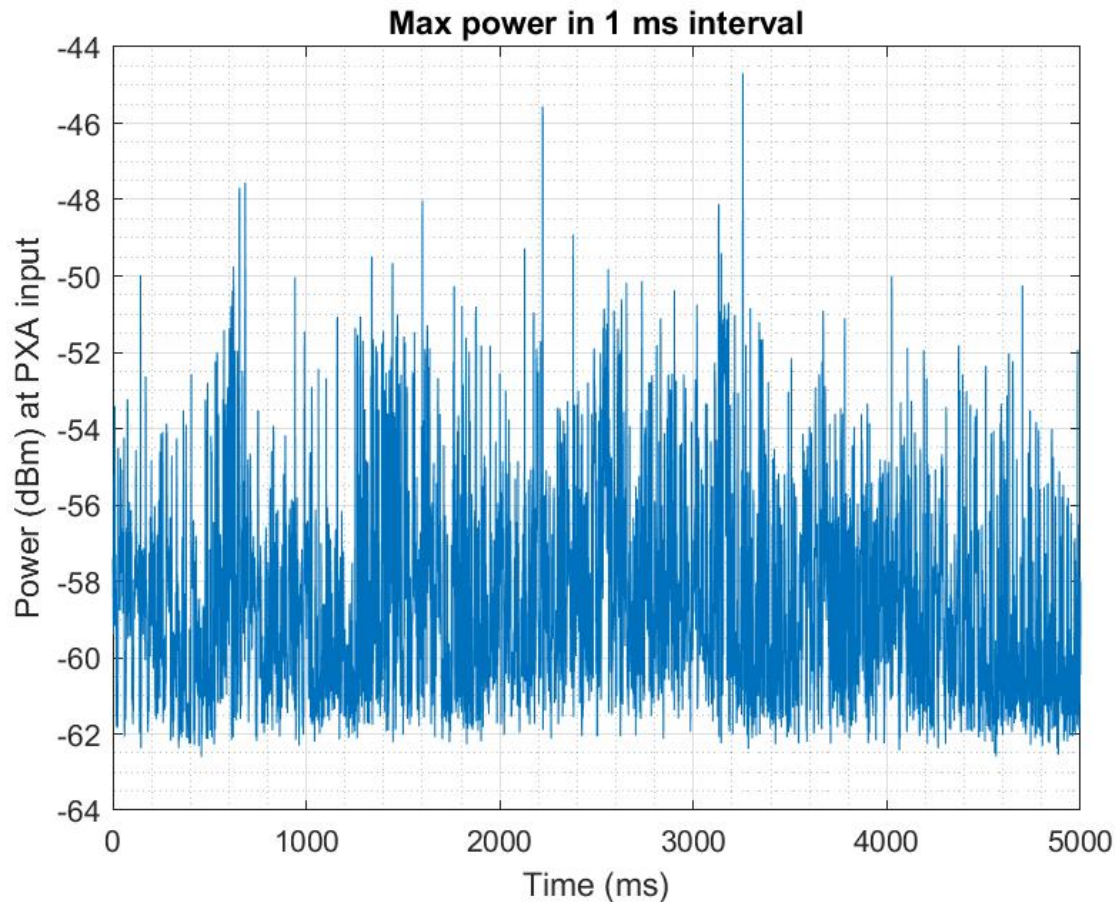


Figure 13. Channel power vs. time plot for a typical capture.

To facilitate a rapid assessment of the signal to noise ratio achieved in each capture we also generated a spectrum contour plot, Figure 14, which summarizes the power statistics for each subcarrier over the full time duration of a capture. Figure 14 shows a companion spectrum contour for the Figure 12 spectrogram and Figure 13 power vs. time plots. Spectrum contour plots were generated from the FFT arrays by computing the cumulative density function for power for each of the 3072 FFT bins and plotting their decile contours at values ranging from 10% to 100%. Note that only the center 2400 bins corresponding to the 36 MHz displayed span are shown in the spectrum contour plots.

The uppermost trace, then, represents the peak power in each 15 kHz bin for the duration of the capture. In the absence of adjacent band emissions we expect the guard bands to exhibit additive white Gaussian noise (AWGN) characteristics due to the noise contributions of the measurement system itself. Therefore, an initial glance at peak signal to average noise may be obtained by relating the uppermost trace to the 60% contour line, since the mean power of Gaussian noise occurs at the 63.2 percentile. Referencing Figure 14 as an example, we observe a peak power of approximately -62 dBm/15 kHz and a mean noise power (in the upper adjacent band) of approximately -109.5 dBm/15 kHz, yielding a peak signal to average noise ratio of approximately 47.5 dB.

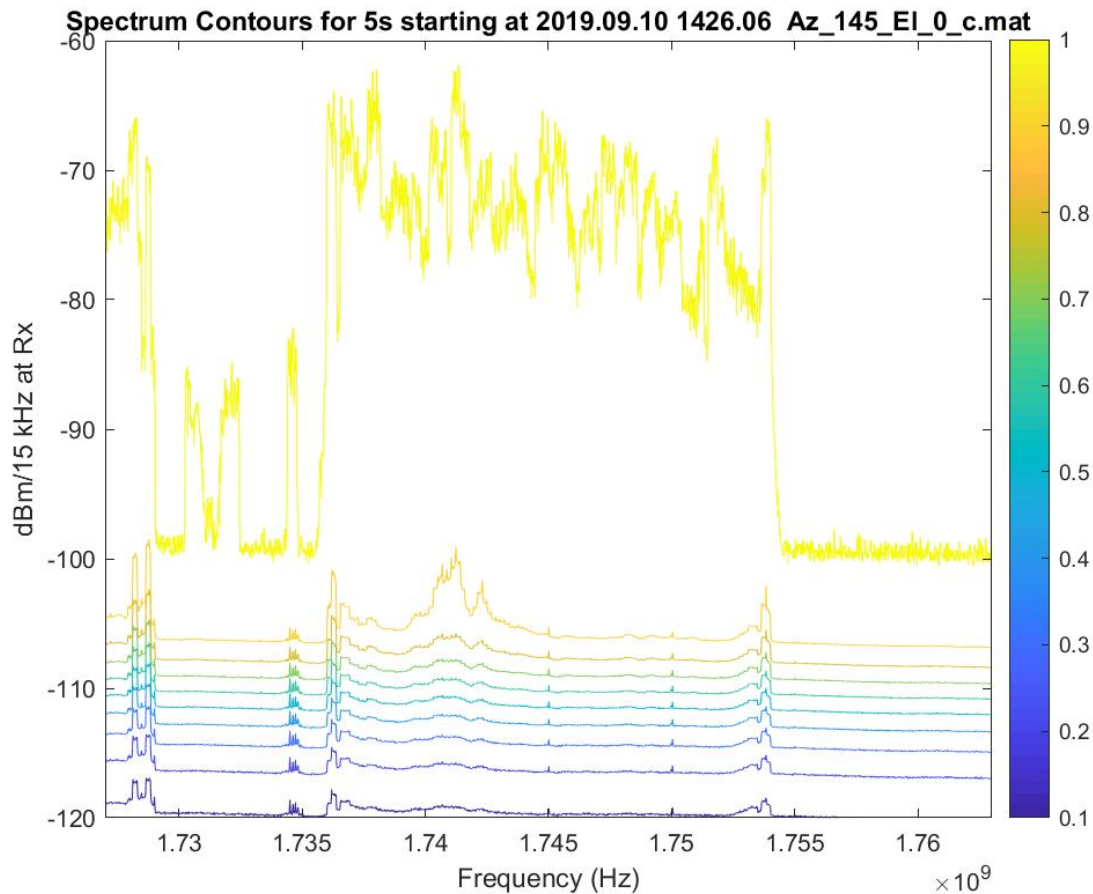


Figure 14. Typical spectrum contours plot for a 5 s timeframe.

1.6 Selection of Waveforms for Bench Testing

1.6.1 Multi-UE Waveforms

To assist in identifying segments of multi-UE (azimuthal) captures to be used in AMT receiver susceptibility bench testing, assessments of the stationarity of channel power, defined as less than ± 3 dB variation over the course of the desired time interval, were developed. Stationarity was a desirable test condition of receiver impact studies of the project, where non-stationary signal structures could lead to uncontrolled upsets in receiver KPI readouts. We used a sliding window technique which involved the following steps:

- 1) Start with the $3072 \times (N/3072)$ FFT array which represents power in mW per 15 kHz bin;
- 2) For each FFT sum linear power across the bins within the 18 MHz occupied bandwidth which in this instance was the center $18,000/15 = 1200$ bins;

- 3) From this result which contains 15 power measurements per ms, compute the cumulative density functions (CDFs) for windows ranging in size from 100-1000 ms or 1500-15000 samples, slid through the data sequence in 50 ms overlapping steps;
- 4) Determine the 50th, 90th, and 99th percentile power for each window; and
- 5) Plot the percentiles as a function of window number.

Figure 15 illustrates the results using a 100 ms window size.

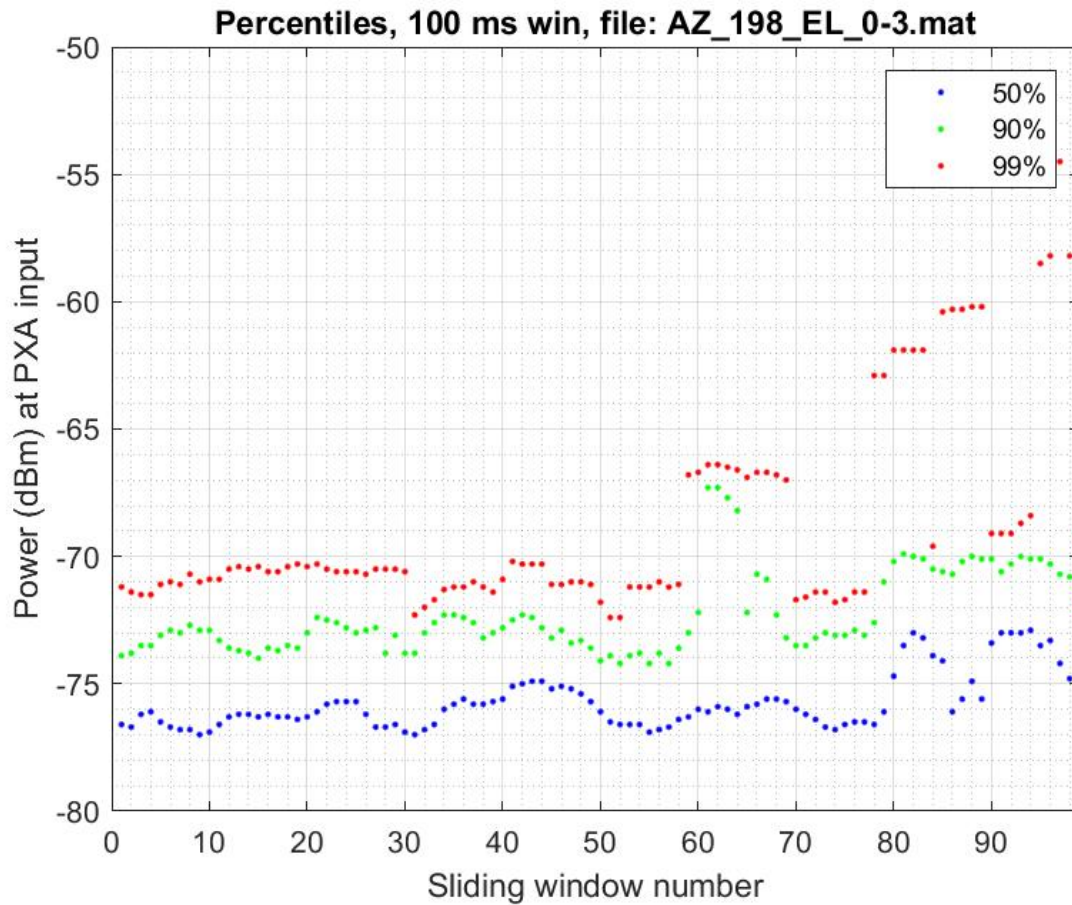


Figure 15. Channel power per FFT for a 100 ms sliding window using 50 ms steps.

We generated plots of this type for window sizes ranging in length from 100-1000 ms to gauge stationarity. Figure 16 shows the results of applying a much larger 500 ms window to the same capture as in Figure 15.

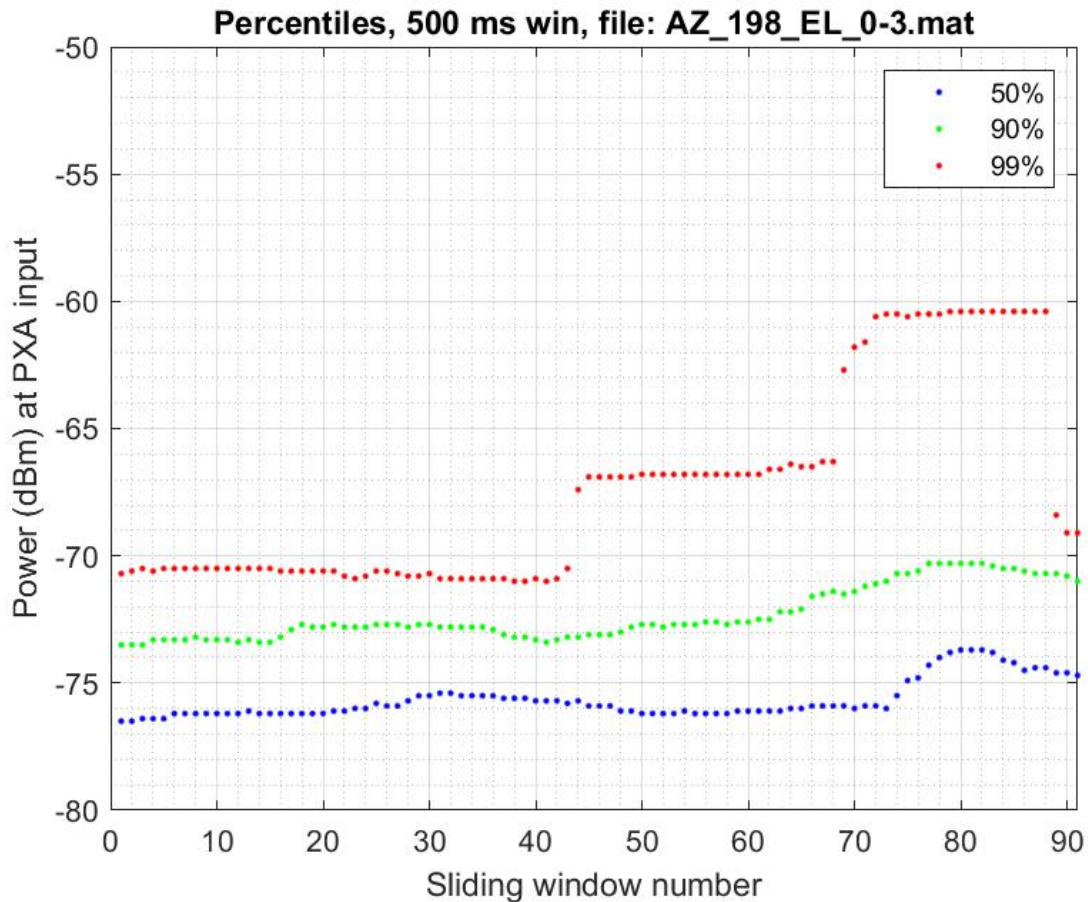


Figure 16. Channel power per FFT for a 500 ms sliding window using 50 ms steps.

We identified captures' minimal playback length suitable for use in bench testing through the following criteria:

- 1) 90th percentile stationarity to be within +/- 3 dB
- 2) Activity in the upper RBs through visual inspection of spectrograms
- 3) In band signal to upper adjacent band noise ratio of at least 20 dB

After investigating the sliding window size for a variety of waveforms we deemed a capture length of 500 ms as a conservative time slice for playback. We selected two captures from each capture site for inclusion in the bench testing effort. Summary graphs of the selected waveforms are shown in Figures 17 to 28.

Selected waveforms from the EAFB site:

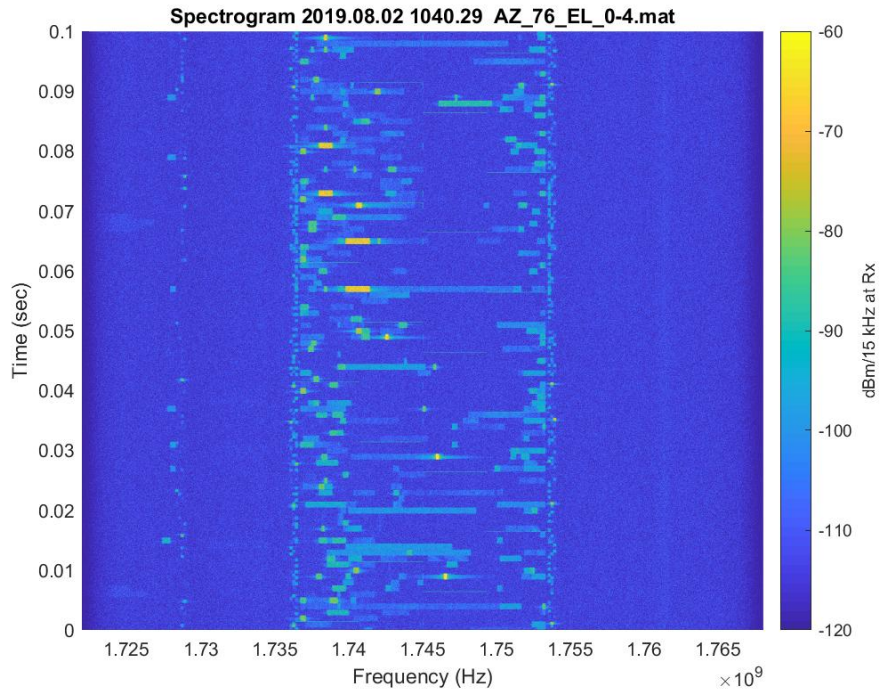


Figure 17. Spectrogram of the first 100 ms in the waveform captured at EAFB along azimuth of 76° .

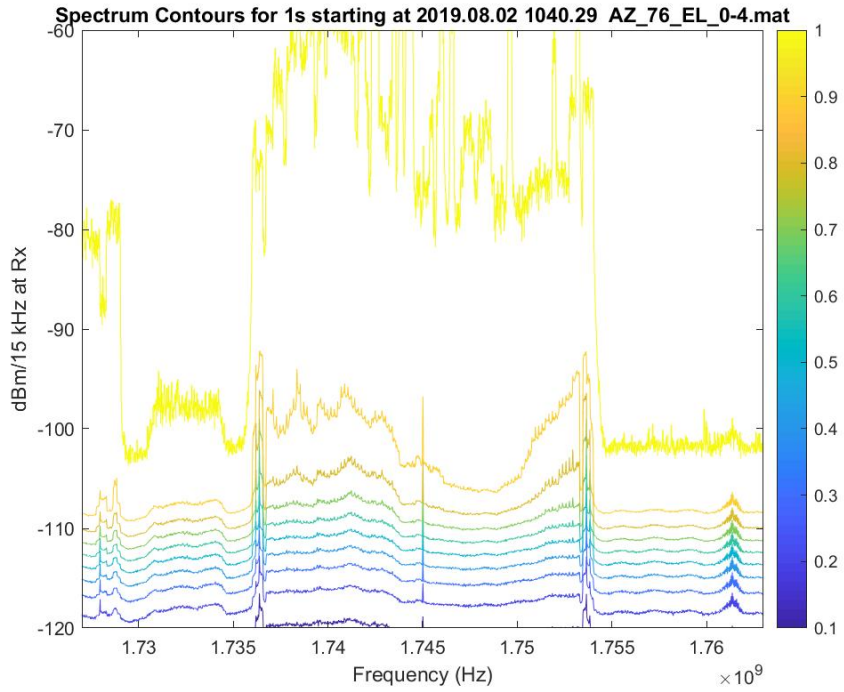


Figure 18. Spectrum contours of the first 1 s in the waveform captured at EAFB along azimuth of 76° .

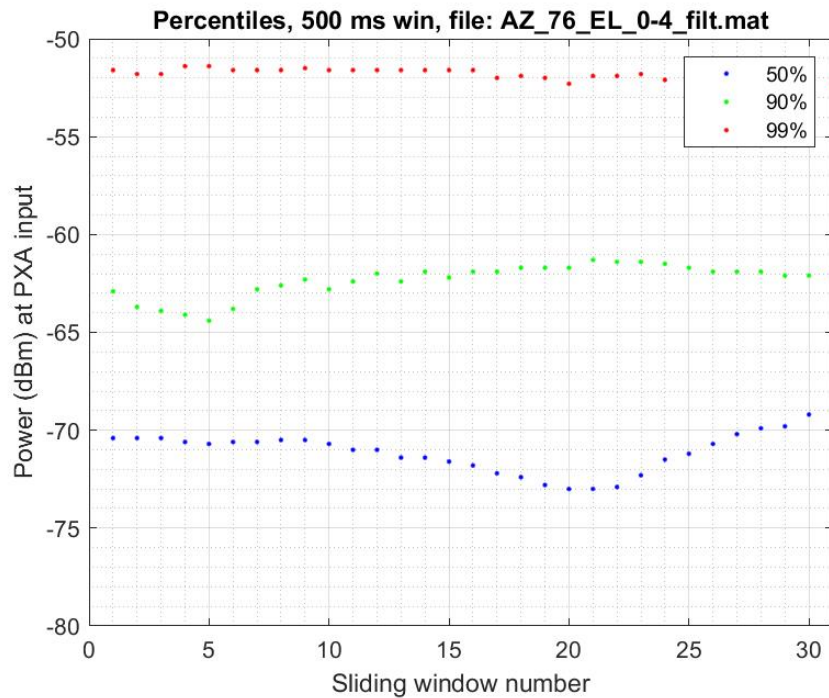


Figure 19. Stationarity analysis, using a 500 ms window size, of the selected waveform captured at EAFB along azimuth of 76° .

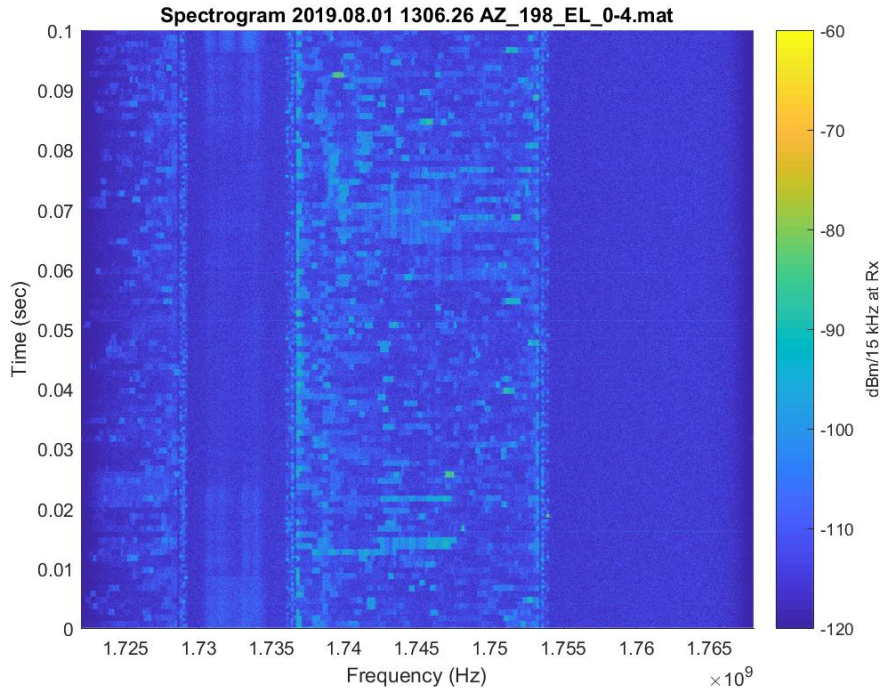


Figure 20. Spectrogram of the first 100 ms in the waveform captured at EAFB along azimuth of 198°.

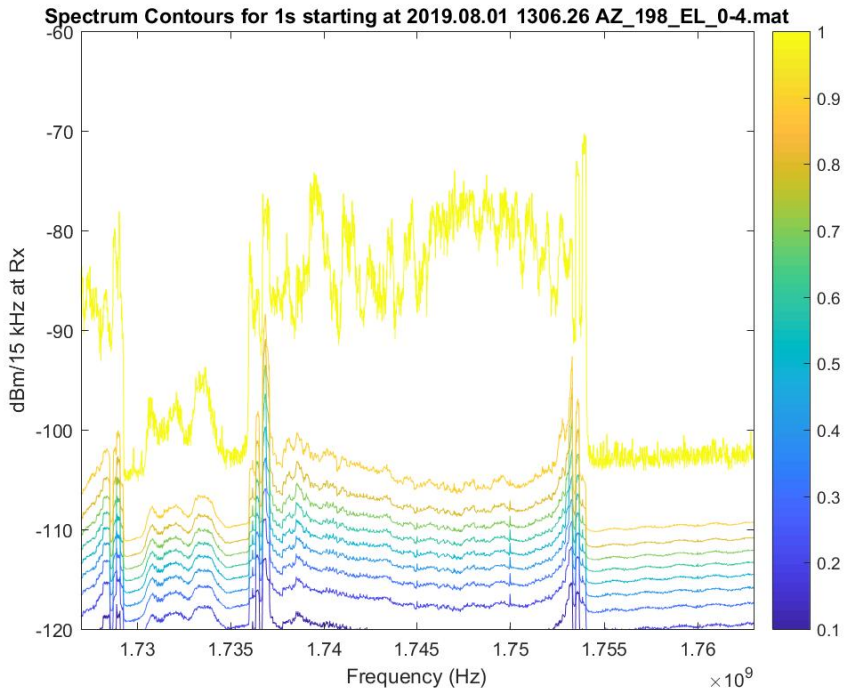


Figure 21. Spectrum contours of the first 1 s in the waveform captured at EAFB along azimuth of 198°.

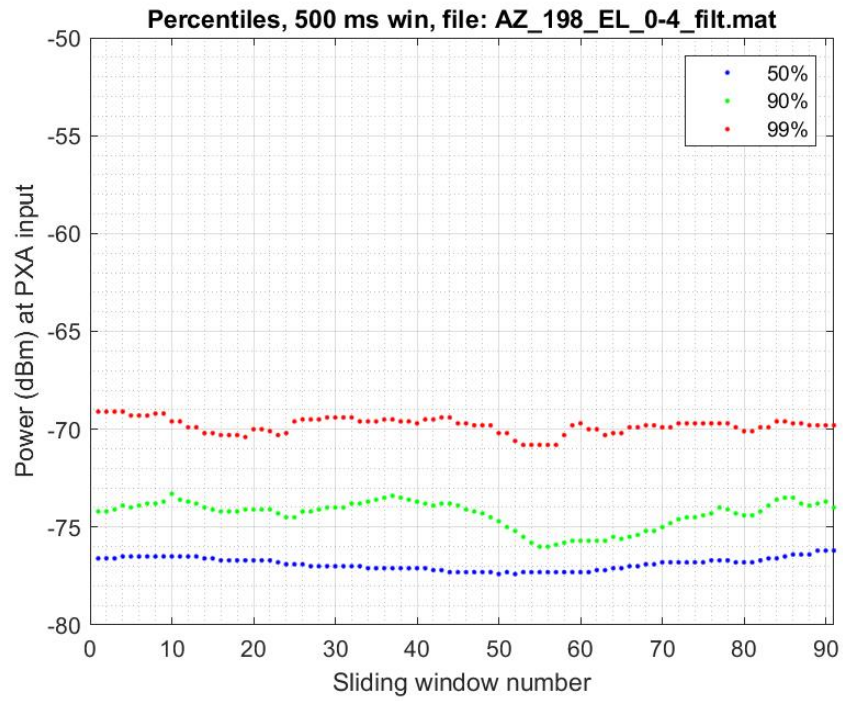


Figure 22. Stationarity analysis, using a 500 ms window size, of the selected waveform captured at EAFB along azimuth of 198°.

Captures selected from the NASA/LaRC Site are shown in Figures 23 through 28. Additional captures chosen for subsequent analysis are shown in the Appendix.

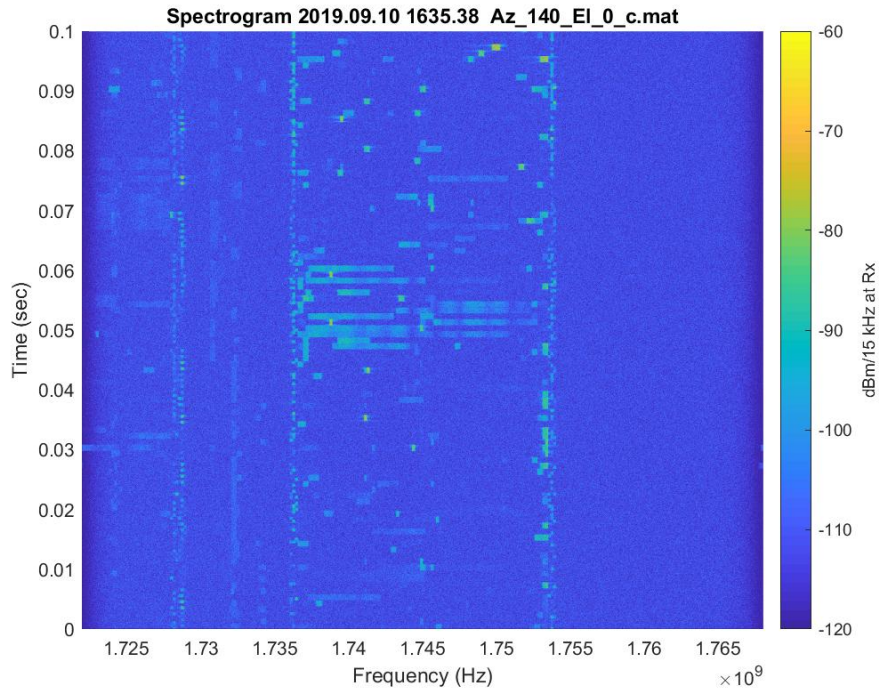


Figure 23. Spectrogram of the first 100 ms in the waveform captured at NASA/LaRC along azimuth of 140°.

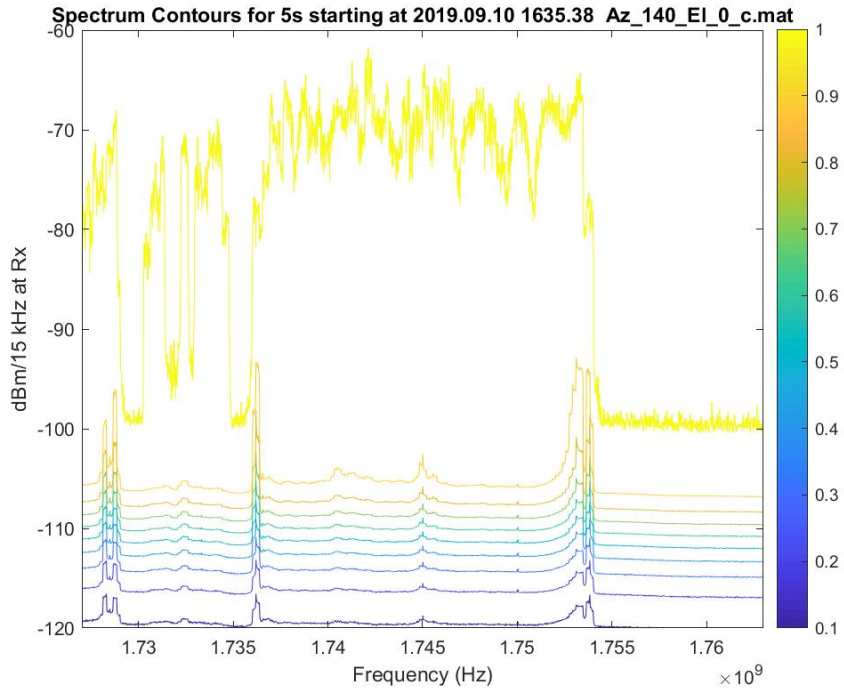


Figure 24. Spectrum contours of the full waveform 5 s captured at NASA/LaRC along azimuth of 140°.

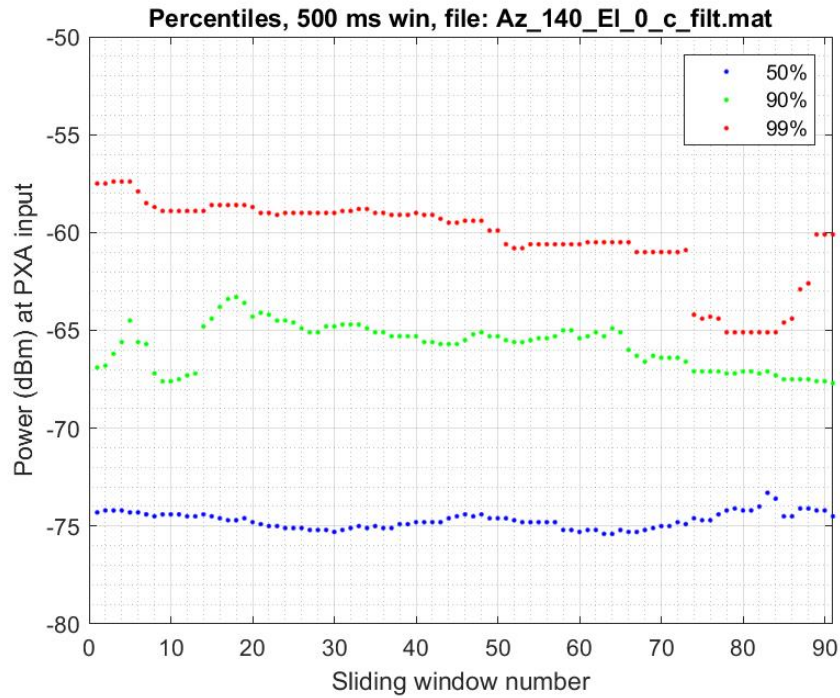


Figure 25. Stationarity analysis, using a 500 ms window size, of the selected waveform captured at NASA/LaRC along azimuth of 140°.

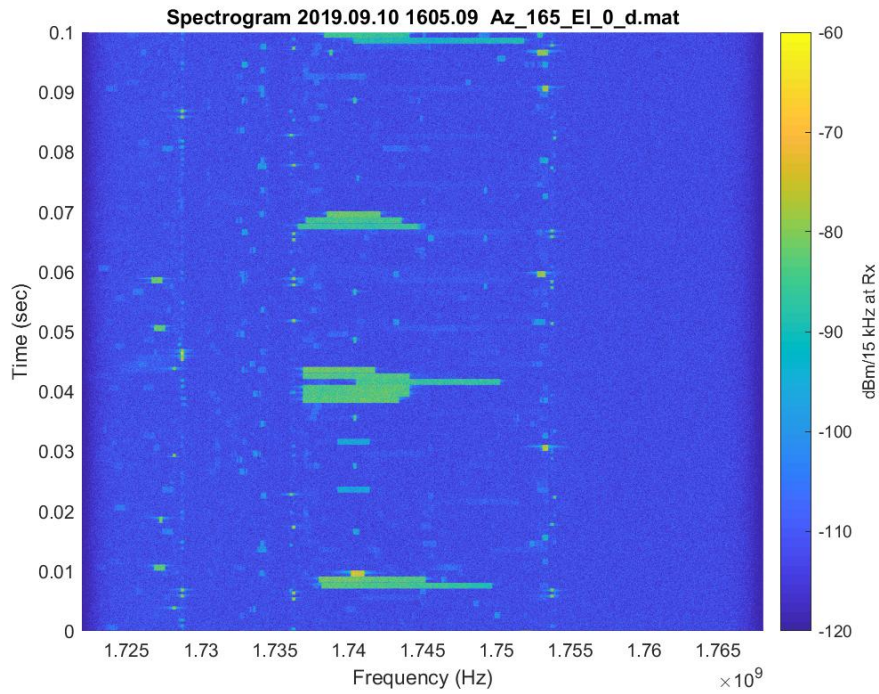


Figure 26. Spectrogram of the first 100 ms in the waveform captured at NASA/LaRC along azimuth of 165°.

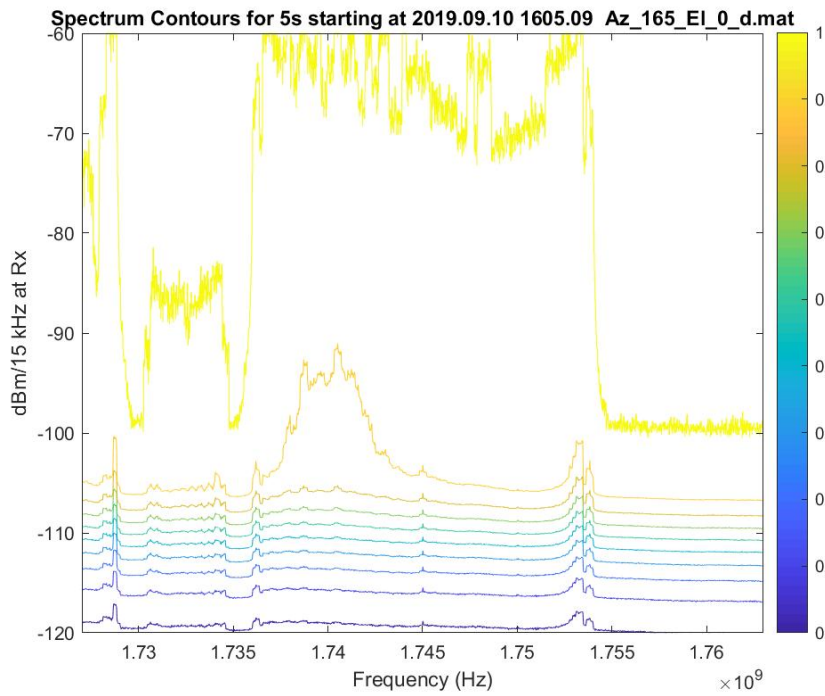


Figure 27. Spectrum contours of the full waveform 5 s captured at NASA/LaRC along azimuth of 165°.

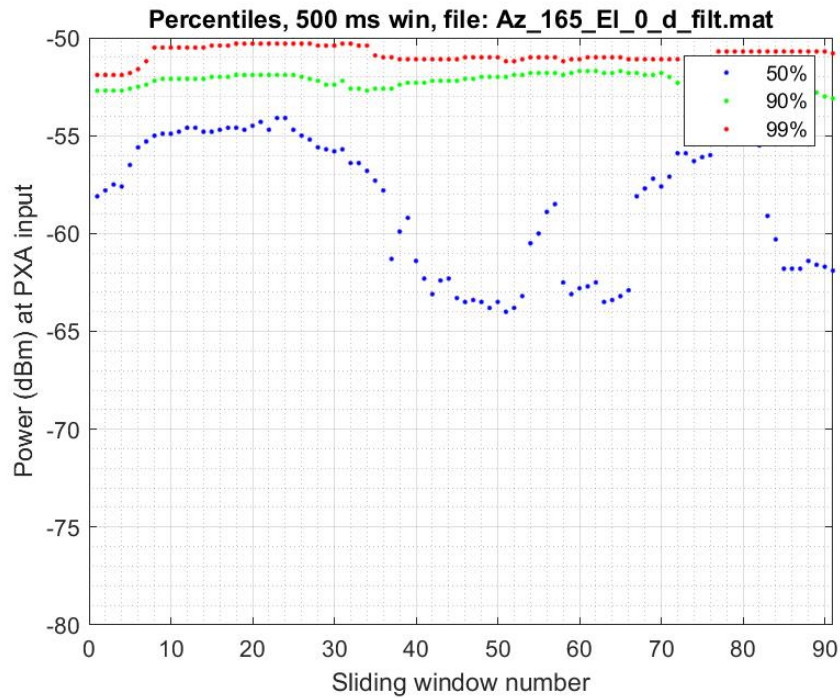


Figure 28. Stationarity analysis, using a 500 ms window size, of the selected waveform captured at NASA/LaRC along azimuth of 165°.

1.6.2 Single UE Waveforms

The test team selected one single UE waveform capture from EAFB to be included in the receiver susceptibility testing. The waveform exhibited a UE upload rate of 10 Mbps, and its summary plots are below:

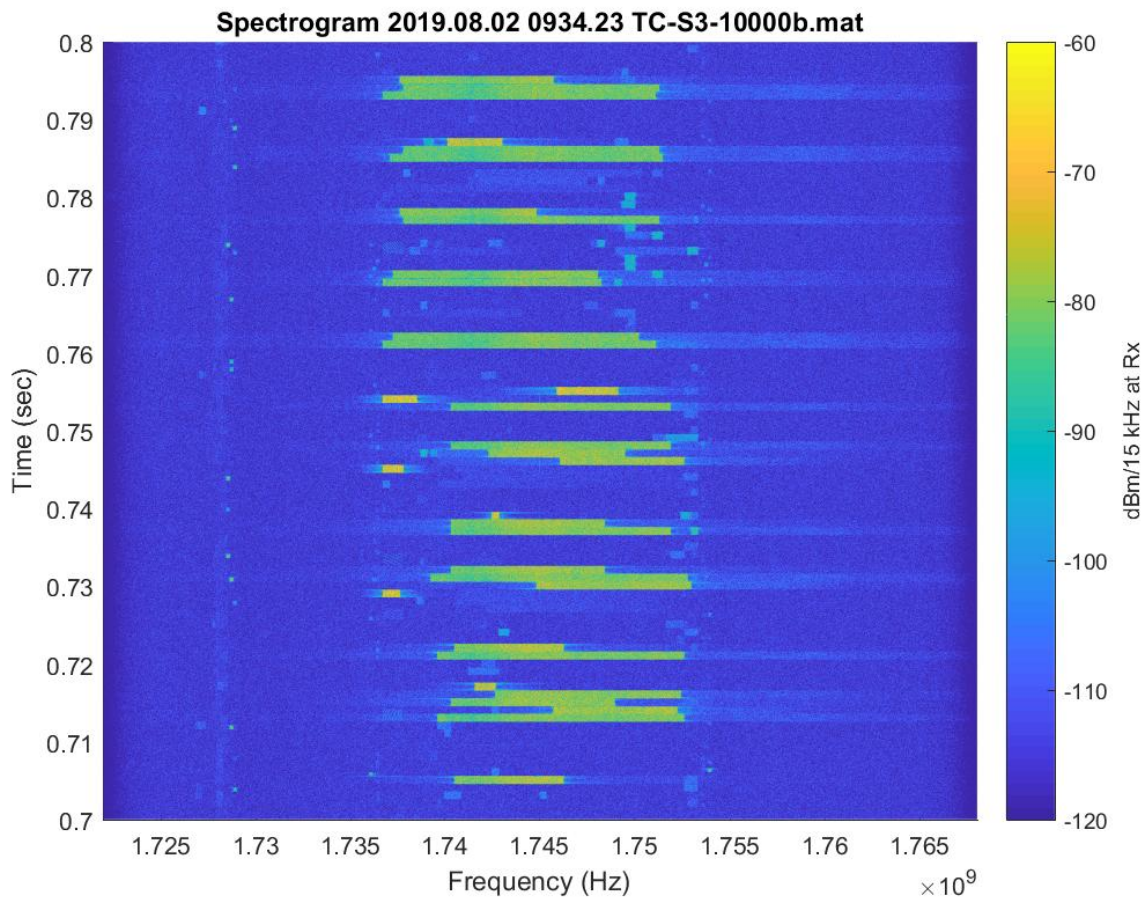


Figure 29. Spectrogram slice of time 0.7s to 0.8 s within the overall 5 s capture of a single UE waveform captured at EAFB. The UE was set to a targeted upload rate of 10 Mbps.

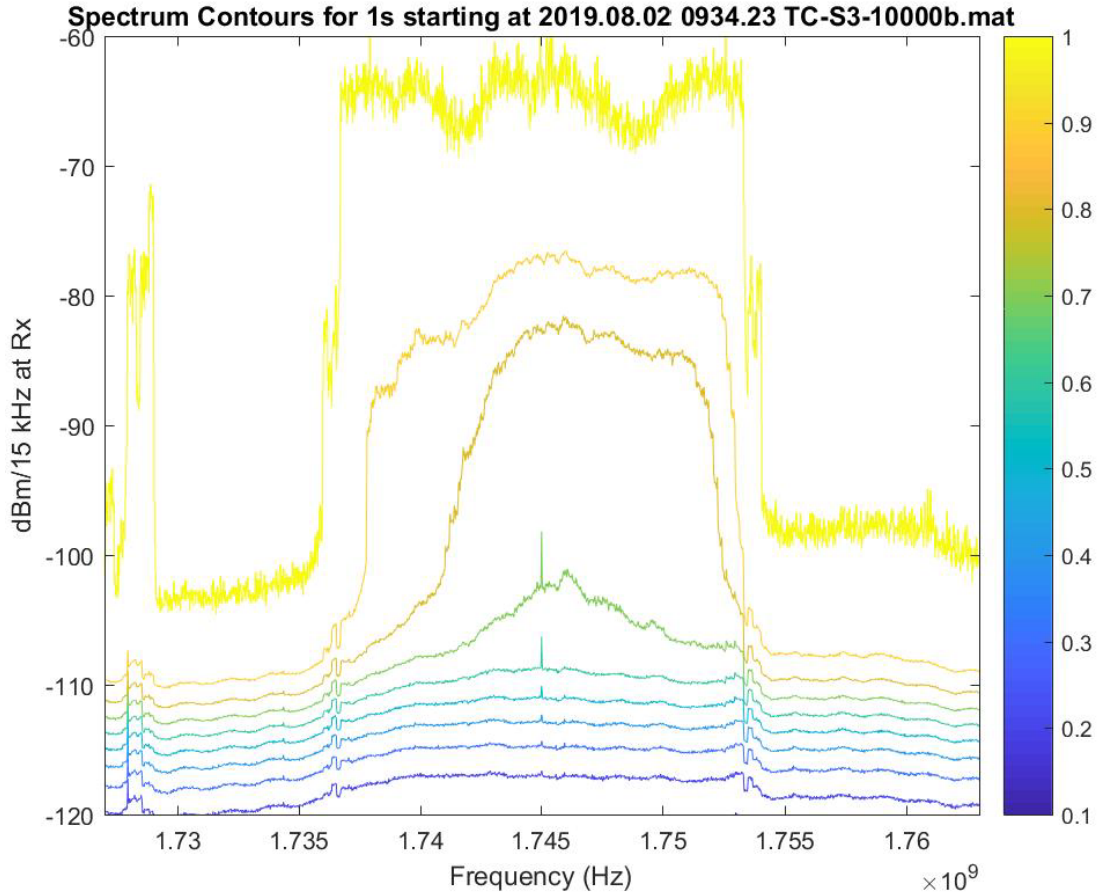


Figure 30. Spectrum contours for the first second of the overall capture.

1.7 Further Signal Analysis Considerations

Since full bandwidth captures include LTE transmissions in the lower adjacent band, which complicates the computation of in-band channel power, they were first bandpass filtered. Since captures were centered on the band of interest this is readily accomplished by filtering the complex waveform using a lowpass FIR filter with 0.2 dB passband ripple, a 9 MHz passband frequency, and 65 dB of stopband attenuation in 1 MHz. Figure 31 shows the filter characteristics while Figure 32 shows the effect of such filtering in a spectrogram plot.

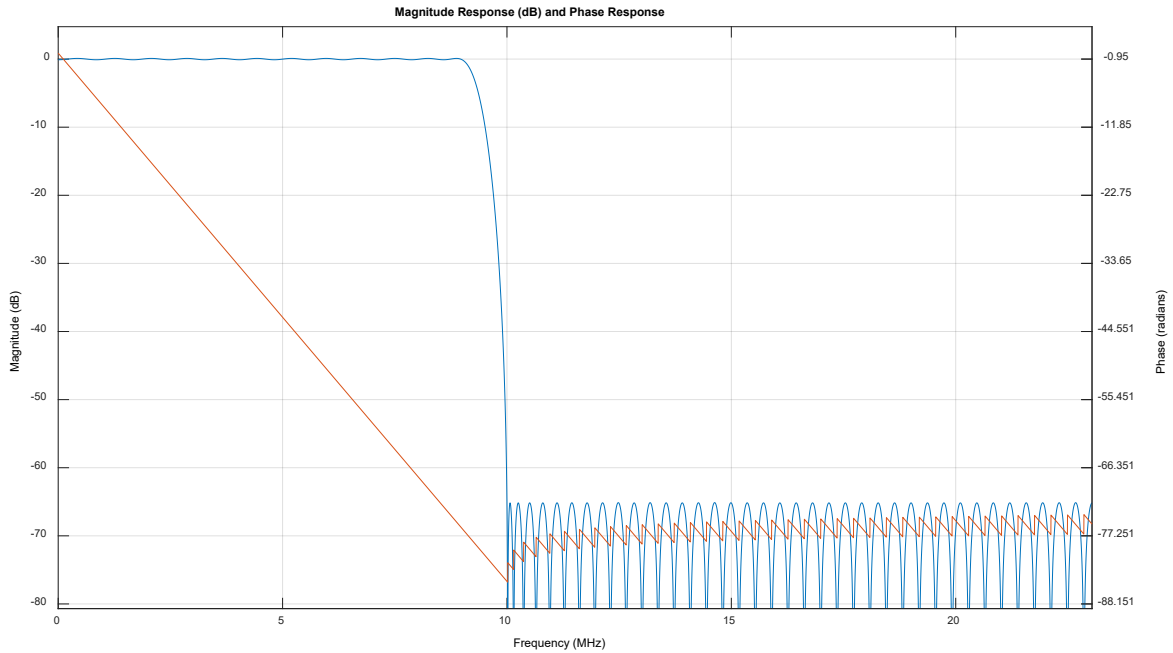


Figure 31. Characteristics of lowpass filter.

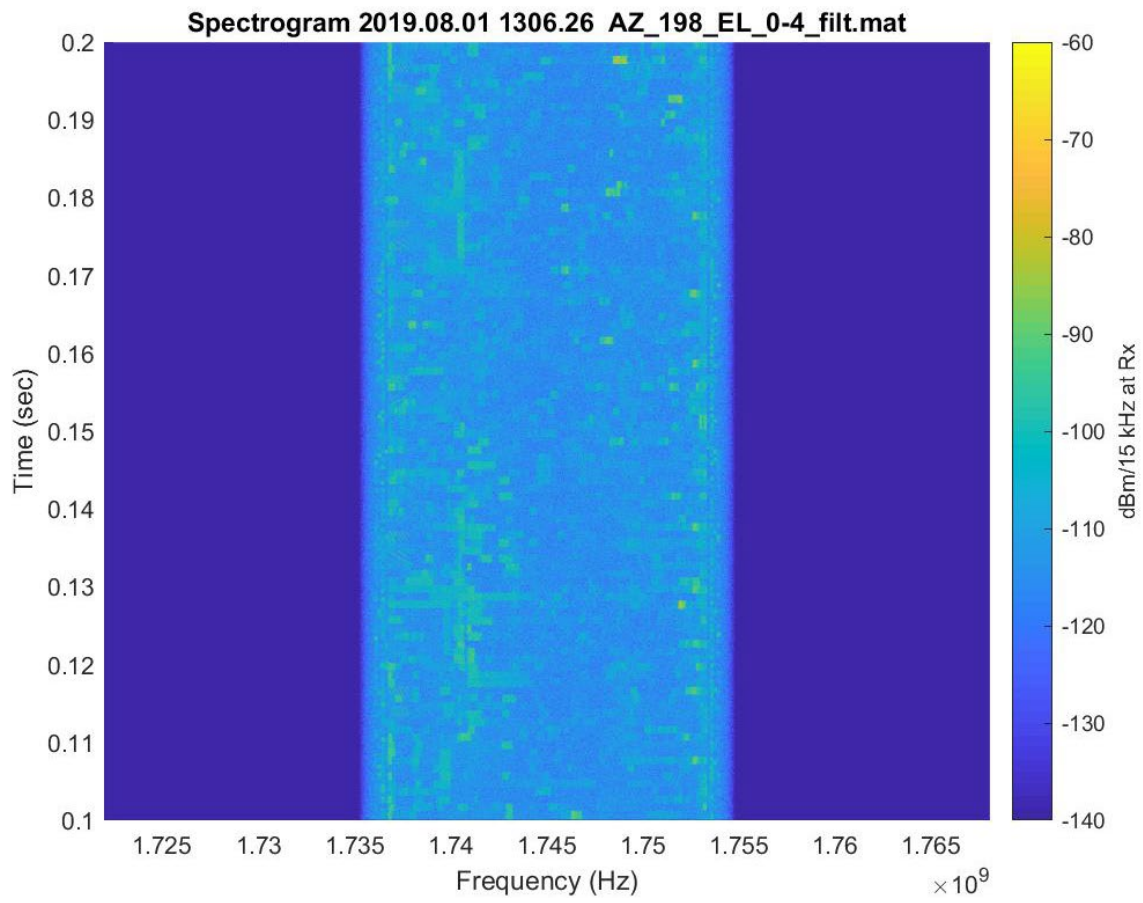


Figure 32. Full bandwidth spectrogram after bandpass filtering.

2. CONCLUSIONS

We present here a technique for recording LTE UE uplink emissions in the AWS-1 band through AMT assets and metrics for selection of I/Q captures as test artifacts suitable for subsequent bench testing. Since wireless carrier deployments in the AWS-1 band are more mature, their existing band occupancy should serve as a proxy for AWS-3 activity in future years. Since they are baseband waveforms, they may be frequency translated using vector signal generators (VSGs) into the AWS-3 frequency range to mimic UE emissions at the upper end of that band, which is adjacent to AMT operations.

Performing in situ measurements using AMT parabolic dish antennas and front end LNAs at EAFB and NASA/LaRC provided multiple benefits. First, they offered sufficient gain to achieve required signal to noise ratios for optimal RTSA captures. As well, the antennas' narrow beamwidths reduced the observed area occupied by UEs, which replicates real world scenarios for AMT systems in general. This manifests itself in a dramatic reduction in band occupancy compared to that which would be observed using a wider beamwidth cellular panel antenna, for example. Finally, since G/T was either measured directly or computed for both locations, that figure of merit may be used in conjunction with likely UE source locations and free space path loss computations to calculate hypothetical received signal levels for various UE location scenarios and EIRPs.

With the RTSA's sensitivity set to maximize dynamic range, the occurrence of transient system overloads were not unexpected. Overloads were typically of very short duration—on the order of several milliseconds—and post-processing techniques were developed to identify segments of captures that were affected, so that the remainder of the capture could still be used, if desired.

A sliding window technique was developed for assessing the stationarity of the captures and selecting candidate captures for use in subsequent bench testing and a desired capture playback duration. The final criteria resulted in the selection of five multiple UE captures and one single UE capture for bench testing.

3. REFERENCES

- [1] E. D. Nelson, "LTE Uplink Aggregate Interference Measurement System," NTIA Technical Memorandum TM-21-552, February 2021, <https://www.its.bldrdoc.gov/publications/3261.aspx>.
- [2] Otis M. Solomon, Jr, *PSD Computations Using Welch's Method*, Sandia Report SAND91-1533, December 1991, available at <https://www.osti.gov/servlets/purl/5688766/>.
- [3] Recommendation ITU-R S.733-2 (2000), *Determination of the G/T ratio for earth stations operating in the fixed-satellite service*, International Telecommunication Union, Geneva, Switzerland, available at <https://www.itu.int/rec/R-REC-S.733/en>.

Appendix A: Waveform Examples

A.1 Selected Waveforms from the Edwards AFB (EAFB) Site

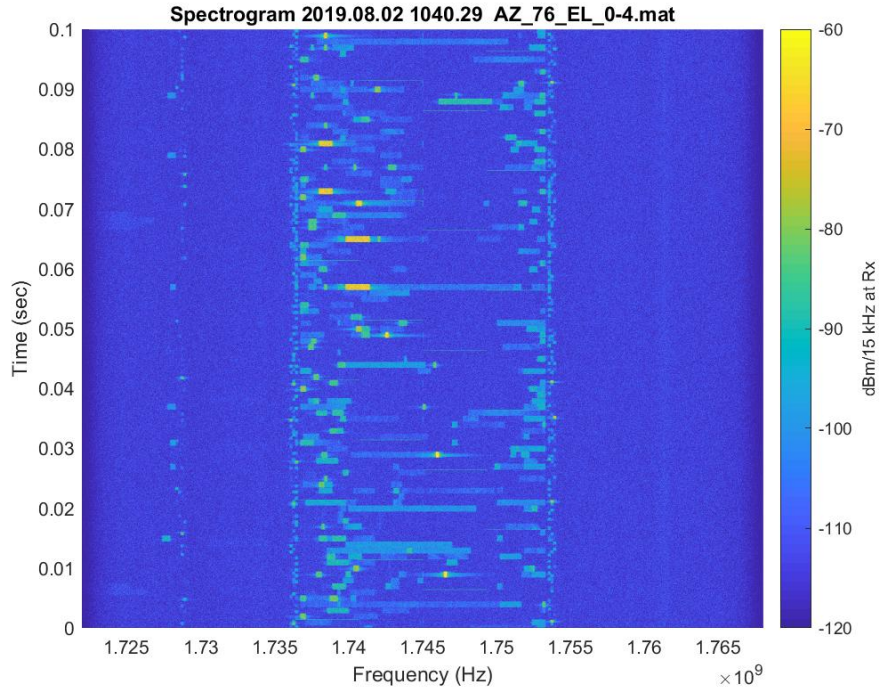


Figure A-1. Spectrogram of the first 100 ms in the waveform captured at EAFB along azimuth of 76° .

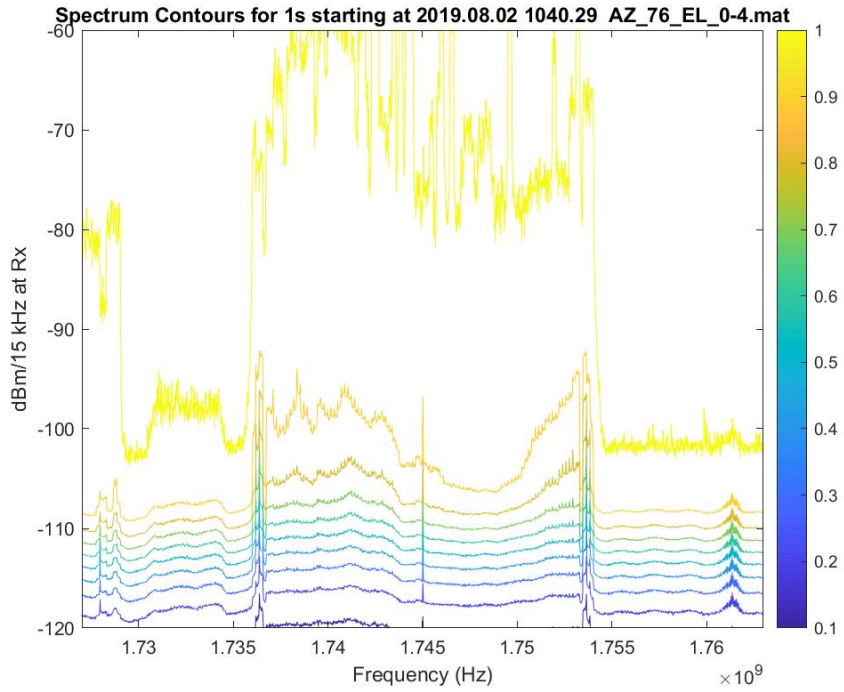


Figure A-2. Spectrum contours of the first 1 s in the waveform captured at EAFB along azimuth of 76°.

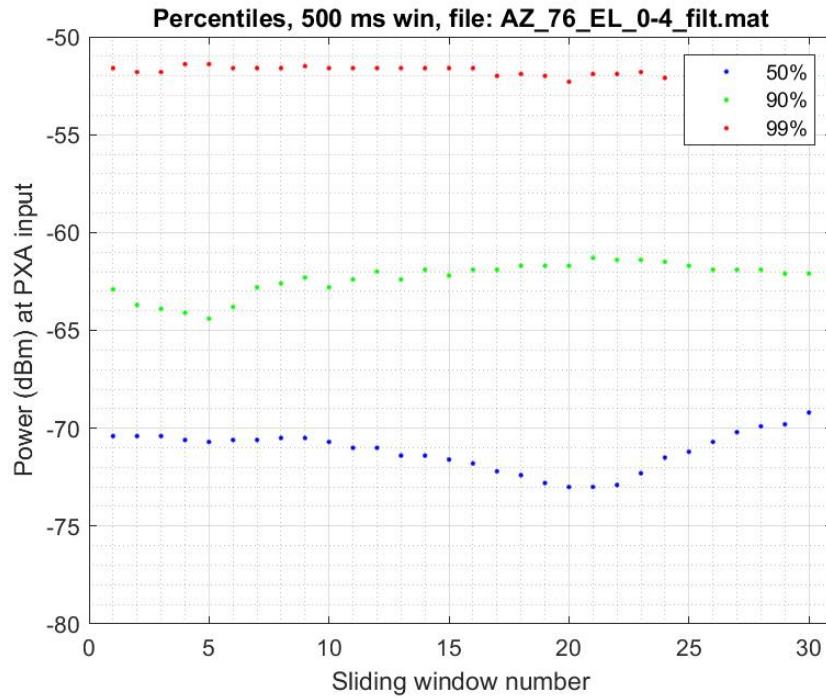


Figure A-3. Stationarity analysis, using a 500 ms window size, of the selected waveform captured at EAFB along azimuth of 76°.

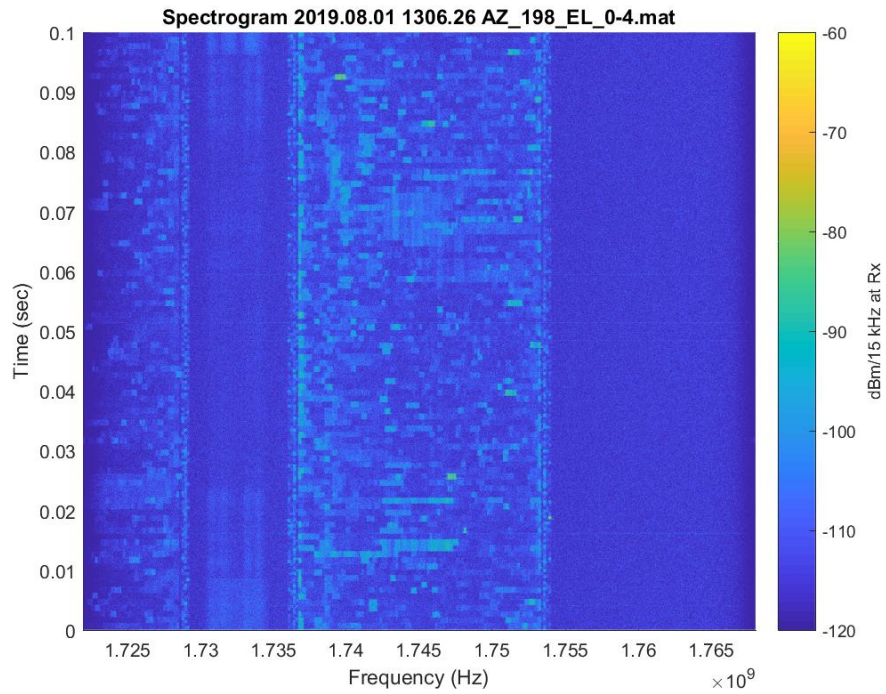


Figure A-4. Spectrogram of the first 100 ms in the waveform captured at EAFB along azimuth of 198°.

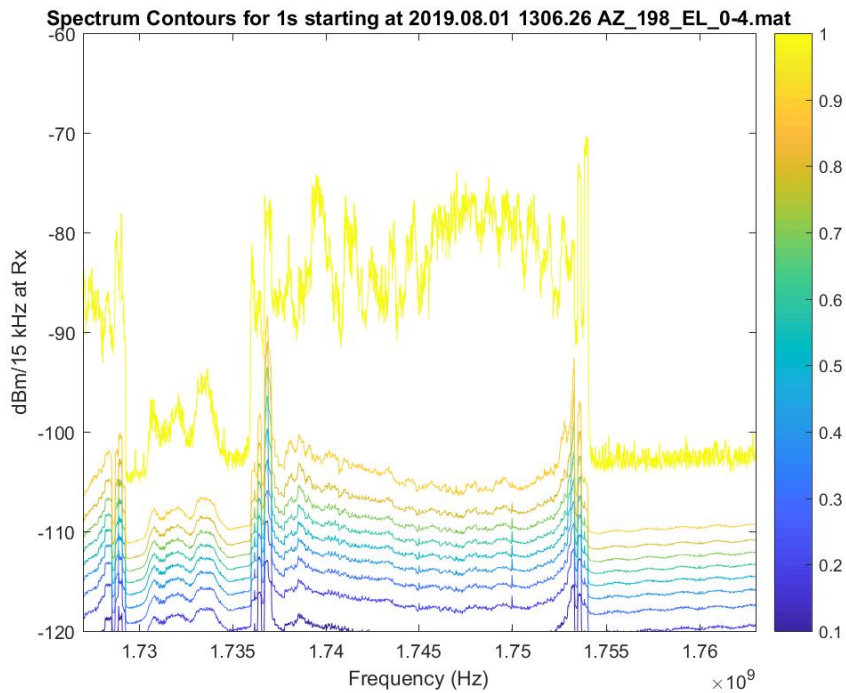


Figure A-5. Spectrum contours of the first 1 s in the waveform captured at EAFB along azimuth of 198°.

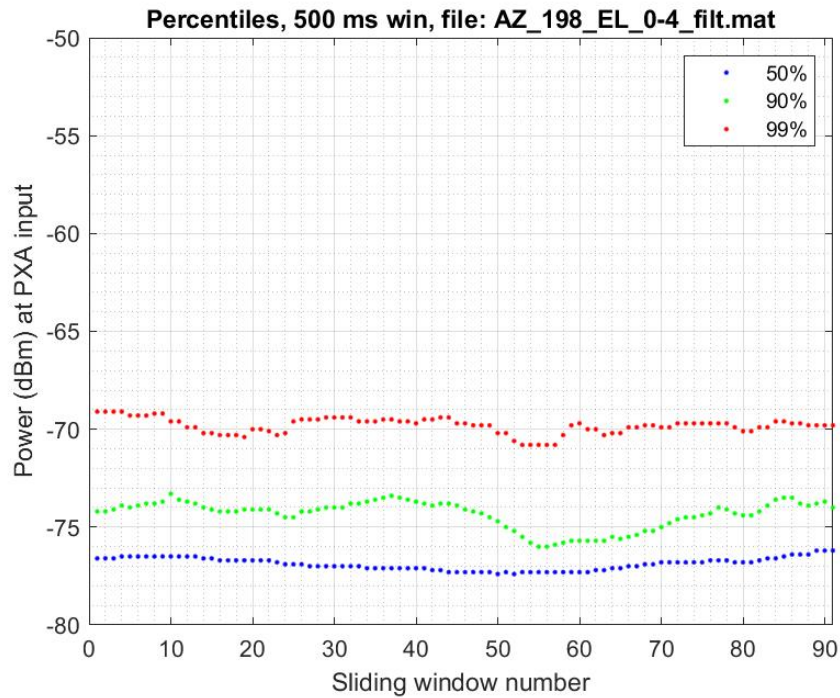


Figure A-6. Stationarity analysis, using a 500 ms window size, of the selected waveform captured at EAFB along azimuth of 198°.

Captures selected from the NASA Langley Research Center (NASA/LaRC) site:

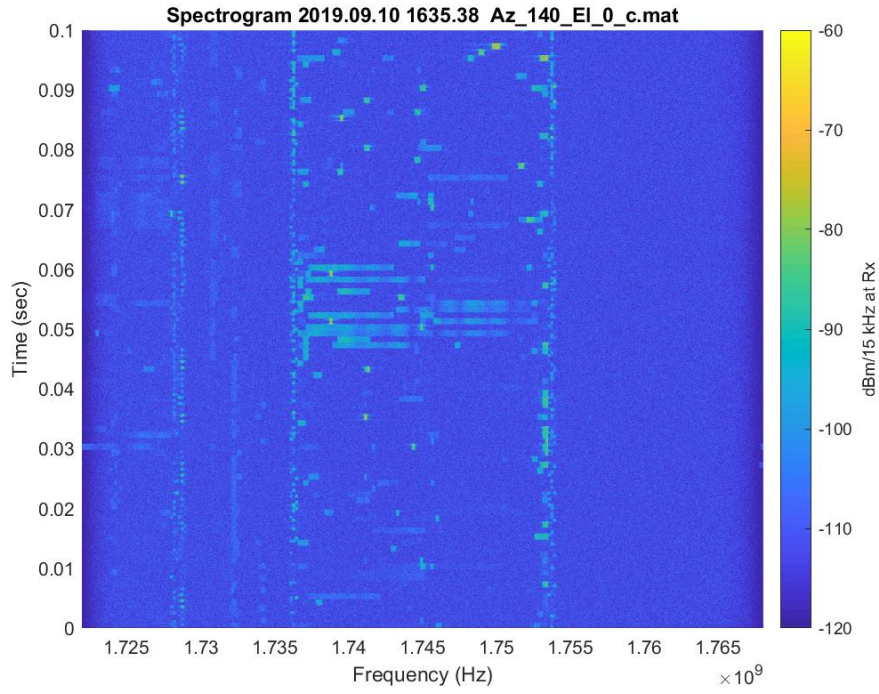


Figure A-7. Spectrogram of the first 100 ms in the waveform captured at NASA/LaRC along azimuth of 140°.

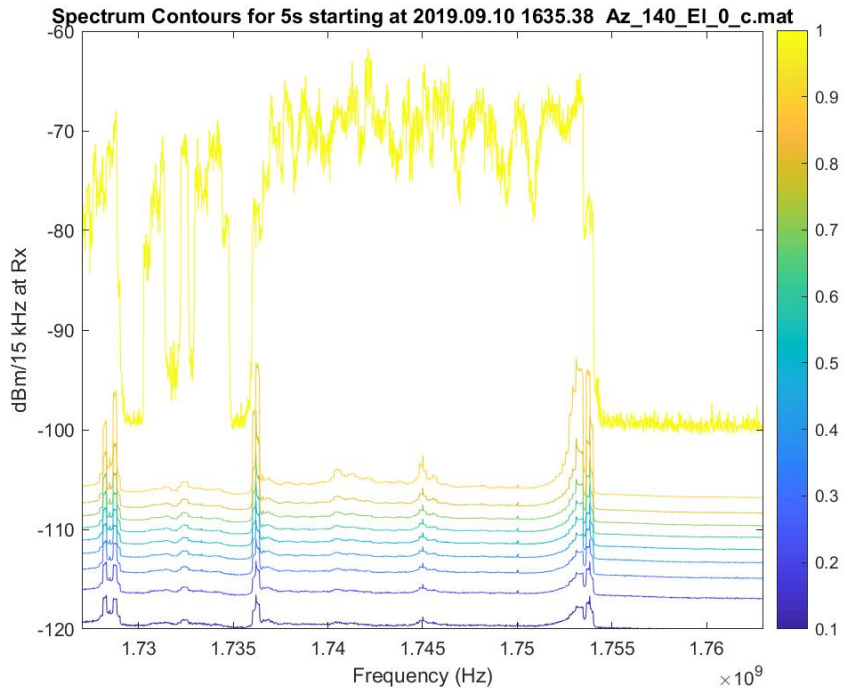


Figure A-8. Spectrum contours of the full waveform 5 s captured at NASA/LaRC along azimuth of 140°.

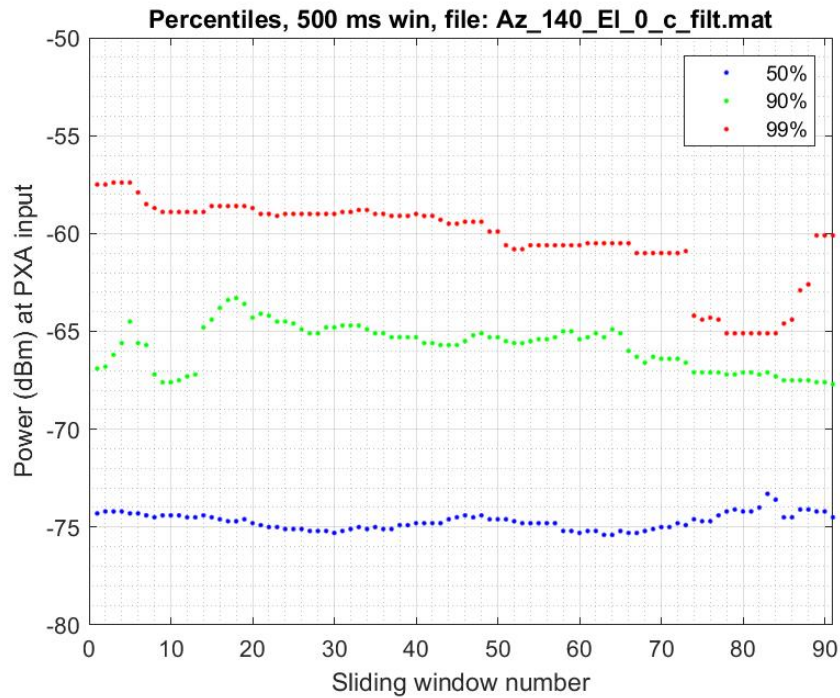


Figure A-9. Stationarity analysis, using a 500 ms window size, of the selected waveform captured at NASA/LaRC along azimuth of 140°.

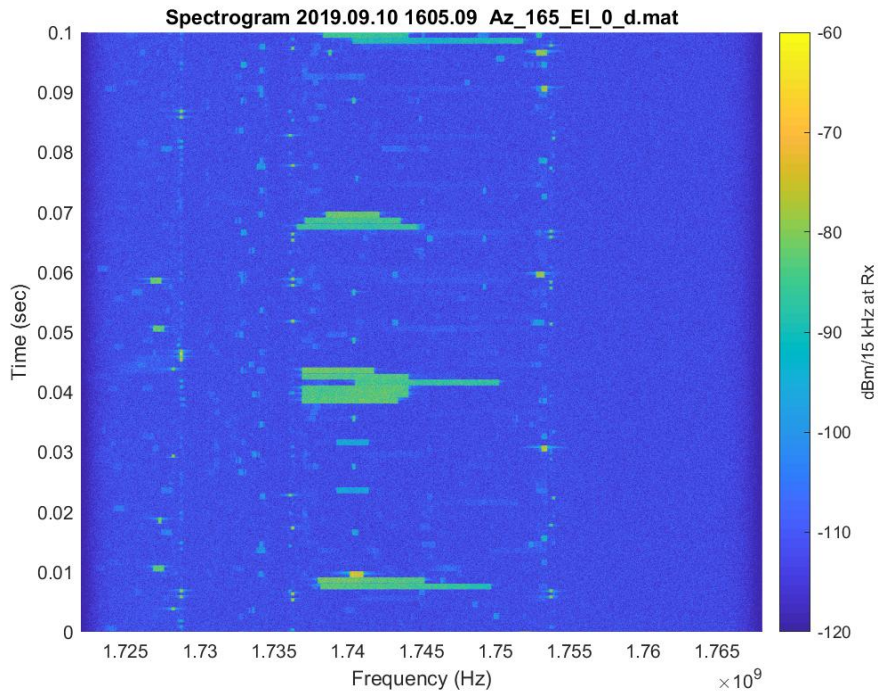


Figure A-10. Spectrogram of the first 100 ms in the waveform captured at NASA/LaRC along azimuth of 165°.

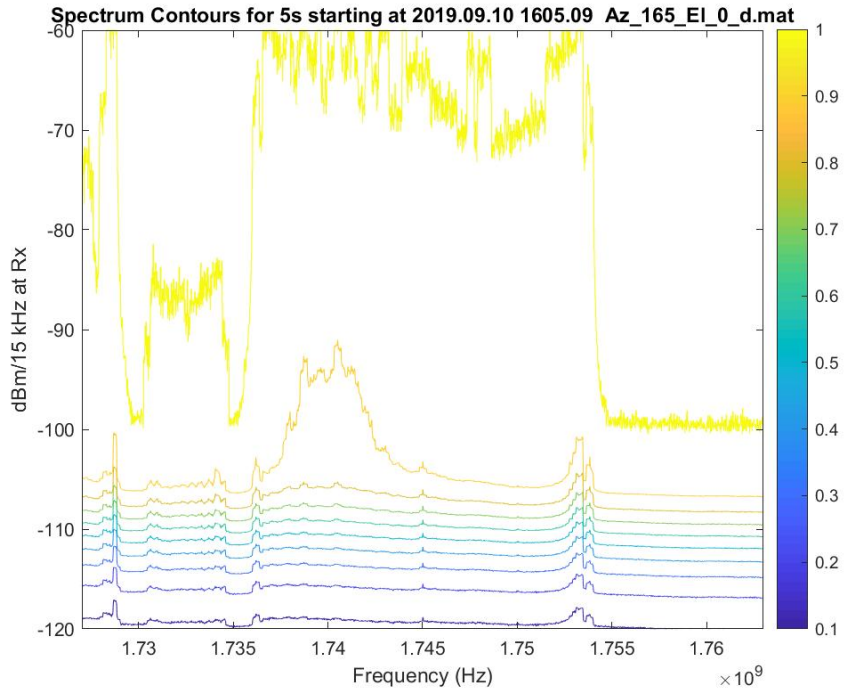


Figure A-11. Spectrum contours of the full waveform 5 s captured at NASA/LaRC along azimuth of 165°.

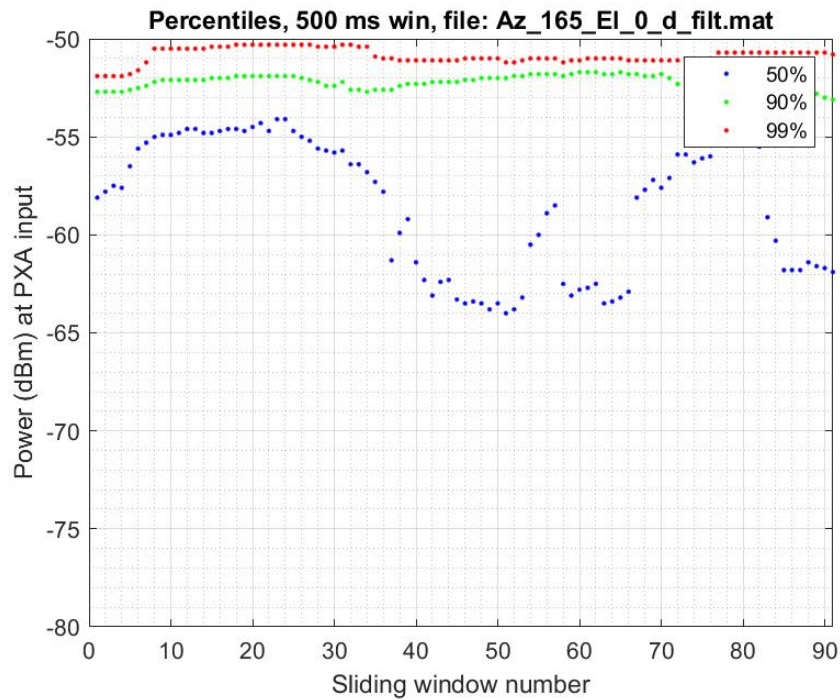


Figure A-12. Stationarity analysis, using a 500 ms window size, of the selected waveform captured at NASA/LaRC along azimuth of 165°.

A.2 Single UE Waveforms

The test team selected one waveform from EAFB to be included in the receiver susceptibility testing. The waveform exhibited a UE upload rate of 10 Mbps, and its summary plots are below:

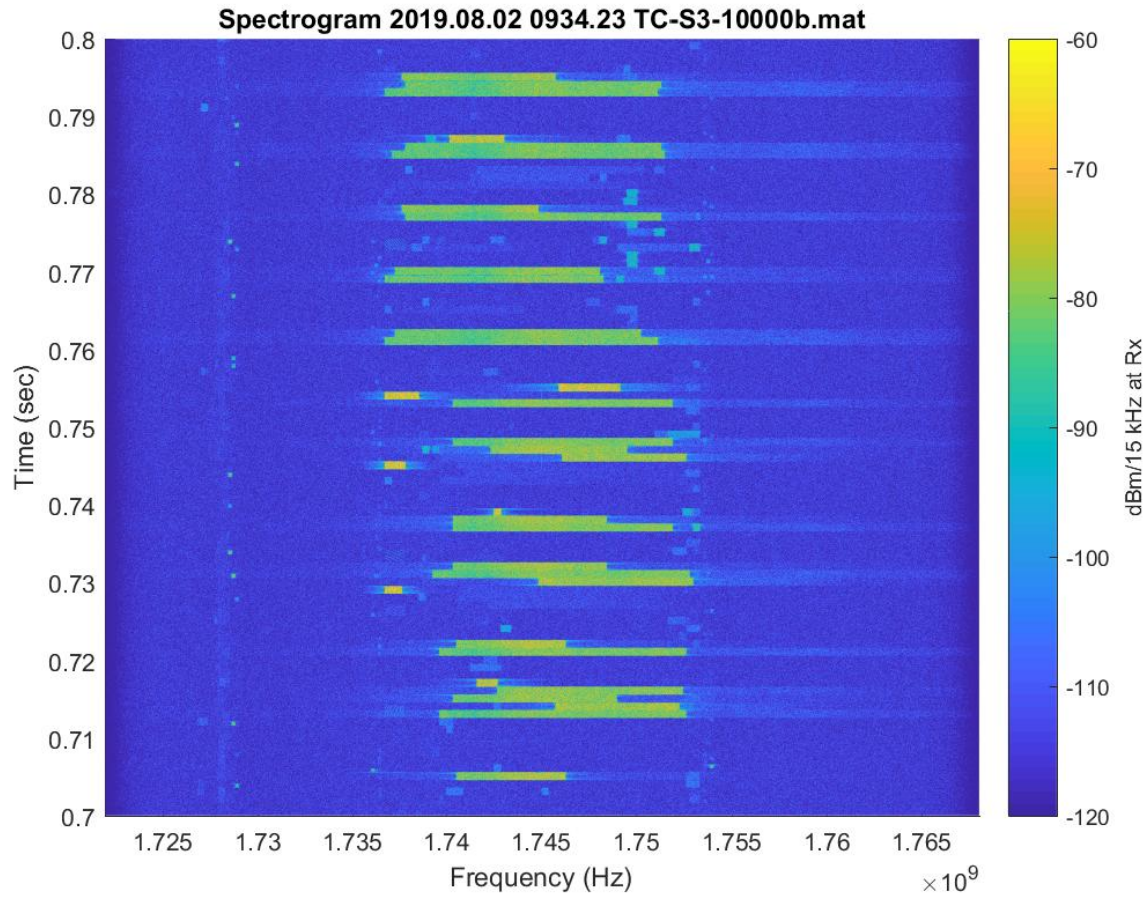


Figure A-13. Spectrogram slice of time 0.7s to 0.8 s within the overall 5 s capture of a single UE waveform captured at EAFB. The UE was set to a targeted upload rate of 10 Mbps.

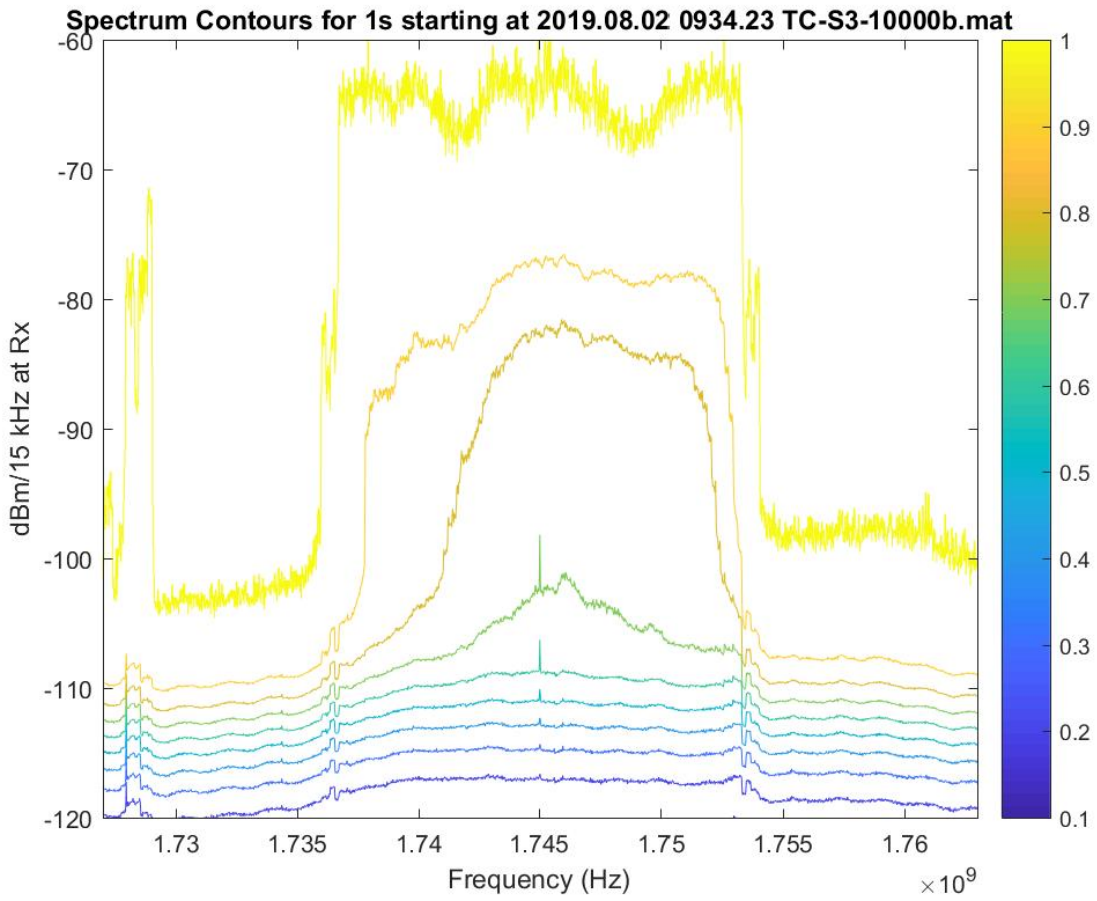


Figure A-14. Spectrum contours for the first second of the overall capture.

BIBLIOGRAPHIC DATA SHEET

| | | |
|---|---|--|
| 1. PUBLICATION NO. TR-21-553 | 2. Government Accession No. | 3. Recipient's Accession No. |
| 4. TITLE AND SUBTITLE In-Situ Captures of AWS-1 LTE for Aeronautical Mobile Telemetry System Evaluation | | 5. Publication Date March 2021 |
| | | 6. Performing Organization Code NTIA/ITS.M |
| 7. AUTHOR(S) Eric D. Nelson and Duncan A. McGillivray | | 9. Project/Task/Work Unit No. 6870000-300 |
| | | 10. Contract/Grant Number. |
| 8. PERFORMING ORGANIZATION NAME AND ADDRESS Institute for Telecommunication Sciences National Telecommunications & Information Administration U.S. Department of Commerce 325 Broadway Boulder, CO 80305 | | 12. Type of Report and Period Covered |
| | | 11. Sponsoring Organization Name and Address Edwards Air Force Base 412th Test Engineering Group, Spectrum Relocation Program 307 E Popson Ave, Ste 204 Edwards AFB, CA 93524-1180 |
| 14. SUPPLEMENTARY NOTES | | |
| 15. ABSTRACT (A 200-word or less factual summary of most significant information. If document includes a significant bibliography or literature survey, mention it here.) This report describes the rationale, measurement methods, and analysis techniques for assessing Long Term Evolution (LTE) user equipment (UE) emissions in the Advanced Wireless Services - 1 (AWS-1) uplink band within the observable range of aeronautical mobile telemetry (AMT) installations at Edwards AFB (EAFB) and NASA Langley Research Center (NASA/LaRC). Site surveys and measurements were conducted to understand the AMT receiver systems' radio frequency (RF) characteristics and survey the local spectrum environment's UE activity through antenna azimuthal scans and test instrument bandwidths encompassing in-band and out-of-band emissions. Based on survey findings, select azimuths were revisited and numerous vector signal analyzer in-phase/quadrature (I/Q) captures of uncontrolled multiple UE over-the-air emissions were performed. A single controlled UE operating in a test mode facilitated captures for several data throughput rates of interest. Data post-processing techniques, analysis methods, and qualifying factors used to identify captures for inclusion in subsequent AMT receiver susceptibility bench top studies are detailed. | | |
| 16. Key Words (Alphabetical order, separated by semicolons) azimuthal scans, AWS-1, vector signal analyzer, I/Q capture, spectrogram, uplink emissions, G/T, spectrum contours, stationarity analysis | | |
| 17. AVAILABILITY STATEMENT <input checked="" type="checkbox"/> UNLIMITED. <input type="checkbox"/> FOR OFFICIAL DISTRIBUTION. | 18. Security Class. (This report) Unclassified | 20. Number of pages 57 |
| 19. Security Class. (This page) Unclassified | | 21. Price: |

NTIA FORMAL PUBLICATION SERIES

NTIA MONOGRAPH (MG)

A scholarly, professionally oriented publication dealing with state-of-the-art research or an authoritative treatment of a broad area. Expected to have long-lasting value.

NTIA SPECIAL PUBLICATION (SP)

Conference proceedings, bibliographies, selected speeches, course and instructional materials, directories, and major studies mandated by Congress.

NTIA REPORT (TR)

Important contributions to existing knowledge of less breadth than a monograph, such as results of completed projects and major activities.

JOINT NTIA/OTHER-AGENCY REPORT (JR)

This report receives both local NTIA and other agency review. Both agencies' logos and report series numbering appear on the cover.

NTIA SOFTWARE & DATA PRODUCTS (SD)

Software such as programs, test data, and sound/video files. This series can be used to transfer technology to U.S. industry.

NTIA HANDBOOK (HB)

Information pertaining to technical procedures, reference and data guides, and formal user's manuals that are expected to be pertinent for a long time.

NTIA TECHNICAL MEMORANDUM (TM)

Technical information typically of less breadth than an NTIA Report. The series includes data, preliminary project results, and information for a specific, limited audience.

For information about NTIA publications, contact the NTIA/ITS Technical Publications Office at 325 Broadway, Boulder, CO, 80305 Tel. (303) 497-3572 or e-mail ITSinfo@ntia.gov.